

FOREWORD

This work was conducted by the National Carbon Company, a Division of Union Carbide Corporation under USAF Contract AF 33(616)-6915. This contract was initiated under Project No. 7350 "Refractory Inorganic Non-Metallic Materials", Task No. 735002 "Graphite Materials Development"; Project No. 7381 "Materials Application", Task No. 738102 "Materials Preproduction Process Development"; and Project No. 7-817 "Process Development for Graphite Materials". The work was administrated under the direction of the Directorate of Materials and Processes, Deputy Commander/Technology, Aeronautical Systems Division, with Captain R. H. Wilson, L. J. Conlon and W. P. Conrardy acting as Project Engineers.

Work under this contract has been in progress since May 1, 1960. The work covered in this report was conducted at the Research Laboratory of National Carbon Company, located at Parma 30, Ohio, under the direction of J. C. Bowman, Director of Research, and W. P. Eatherly, Assistant Director of Research.

It is a pleasure to acknowledge the contributions of J. W. McClure and L. B. Smith, who programmed the numerical computations for the LGP-30 electronic computer at the Parma Research Laboratory. The author would like to thank J. W. McClure, J. A. Krumhansl, Charles S. Smith, and R. Smoluchowski for several helpful discussions, and S. Amelinckx for supplying some results prior to publication.

This is the second of a series of volumes of WADD Technical Report 61-72 prepared to describe various phases of the work. The preceding volume of this series is:

Volume I Observations by Electron Microscopy of Dislocations in Graphite, by Richard Sprague.

Contrails

ABSTRACT

Eshelby, Read, and Shockley's theory of dislocations in an anisotropic elastic continuum has been used to derive formulas not involving complex numbers for the stress components of straight dislocations in certain symmetry directions. From these the dependence of stacking fault energy γ_F on the orientation of the Burgers vector and on the width of extended dislocations and triple partial ribbons and the dependence of γ_F on the radius of curvature of extended nodes have been calculated. The results are rigorous for hexagonal crystals and approximate for general directions in (111) planes of FCC crystals. The theory is applied to graphite and close-packed metals. All three methods of determining γ_F for graphite yield results which are compatible with the value 0.6 ± 0.2 erg/cm². The rough estimate of error is based on uncertainties in the elastic constants and differences in experimental results. The dependence of width on depth from the stress-free surface has been calculated for an arbitrarily oriented dislocation lying parallel to the surface of a semi-infinite isotropic body and a 30° extended dislocation and a symmetrical, screw triple partial ribbon in certain symmetry directions in an anisotropic plate. A procedure for correcting the widths observed in electron microscopy of thin films is given.

This report has been reviewed and is approved.



W. G. RAMKE
Chief, Ceramics and Graphite Branch
Metals and Ceramics Laboratory
Directorate of Materials and Processes

TABLE OF CONTENTS

| | PAGE |
|--|------|
| 1. INTRODUCTION AND OBJECTIVES. | 1 |
| 2. DISLOCATIONS IN SYMMETRY DIRECTIONS | 2 |
| 2.1. Derivation of Conditions on the Elastic Constants | 2 |
| 2.2. Displacements, Stresses, and Related Quantities for Type I Elastic Constants | 4 |
| 2.3. Screw Dislocation in an Anisotropic Flat Plate | 11 |
| 3. LINE ENERGY OF DISLOCATIONS | 13 |
| 3.1. Analytical Results | 13 |
| 3.2. Numerical Results | 14 |
| 4. FORCE BETWEEN DISLOCATIONS AND STACKING FAULT ENERGY . 18 | |
| 4.1. Force Between Two Parallel Dislocations | 18 |
| 4.2. Stacking Fault Energy and Width of Extended Dislocations | 21 |
| 4.3. Stacking Fault Energy and Width of Triple Partial Ribbons | 26 |
| 4.4. Stacking Fault Energy and Radius of Extended Nodes | 28 |
| 4.5. Stacking Fault Energy of Graphite | 28 |
| 5. INFLUENCE OF A STRESS-FREE SURFACE ON DISLOCATION WIDTHS | 29 |
| 5.1. Arbitrary Extended Dislocation in a Semi-Infinite Isotropic Solid | 30 |
| 5.2. A 30° Extended Dislocation in an Anisotropic Plate | 32 |
| 5.3. A Symmetrical, Screw Triple Partial Ribbon in an Anisotropic Plate | 37 |
| 6. SUMMARY AND CONCLUSIONS | 40 |
| APPENDIX I - ELASTIC CONSTANTS | 43 |
| I.1. Derivation of Coordinate Systems for Types I and II Elastic Constants | 43 |
| I.2. Examples of Type I Elastic Constants | 44 |
| I.3. Numerical Values of Elastic Constants | 45 |
| BIBLIOGRAPHY. | 47 |

LIST OF ILLUSTRATIONS

| FIGURE | | PAGE |
|--------|--|------|
| 1. | Coordinate system for a dislocation in a flat plate | 11 |
| 2. | Variation of line energy factor K with angle α between dislocation and Burgers vector for $\{111\}$ slip plane | 17 |
| 3. | Schematic drawing of an extended dislocation in the $x_2 x_3$ plane | 19 |
| 4. | Orientation of an extended dislocation in the $\{111\}$ plane | 20 |
| 5. | Schematic drawing of dislocations with equal Burgers vectors | 21 |
| 6. | Stacking fault energy times width of extended dislocation versus orientation | 24 |
| 7. | Approximate value of stacking fault energy times width of extended dislocation versus orientation | 24 |
| 8. | Schematic drawing of a triple partial ribbon | 27 |
| 9. | Coordinate system for an extended dislocation in a semi-infinite solid | 30 |
| 10. | Variation in width of a dislocation in a semi-infinite isotropic solid with depth from surface | 33 |
| 11. | Variation in width of a dislocation in a semi-infinite isotropic solid with depth from surface | 33 |
| 12. | Variation in width of a screw dislocation in a semi-infinite isotropic solid of large ν with depth from surface | 34 |
| 13. | Width of a 30° extended dislocation in a graphite plate versus the parameter Ω | 36 |
| 14. | Width of a 30° extended dislocation in a graphite plate as a function of depth from surface and thickness of plate. | 37 |
| 15. | Width of a symmetrical, screw triple partial ribbon in a graphite plate versus the parameter Ω | 39 |
| 16. | Width of a symmetrical, screw triple partial ribbon in a graphite plate as a function of depth from surface and thickness of plate | 39 |

LIST OF TABLES

| TABLE | | PAGE |
|-------|---|------|
| 1 | Analytical Line Energy Factors for Dislocations | 14 |
| 2 | Numerical Line Energy Factors for Dislocations | 15 |
| 3 | Stacking Fault Energy Times Dislocation Width | 23 |
| 4 | Comparison with Results of Seeger and Schöck for γ_F^w | 25 |
| 5 | Numerical Values for Elastic Constants and Burgers Vectors | 46 |

1. INTRODUCTION AND OBJECTIVES

This work arose from the immediate need of accurate formulas to use in the interpretation of electron micrographs of dislocations in thin films of graphite. That formulas for an isotropic material may not be even approximately correct for graphite is indicated by the anisotropy factor $A = 2c_{55} / (c_{11} - c_{13})$, where the c_{ij} are the elastic stiffness constants. For an isotropic material one finds $A = 1$, for many metals of cubic symmetry $A \approx 3$, but for graphite $A \approx 1/190$. The source of this anisotropy is, of course, the weak binding between layer planes.

Up to the present almost all theoretical work on dislocations has been based on the linear elastic continuum theory of dislocations. A general method for deriving the displacements of atoms and the components of the stress field surrounding a straight dislocation in an infinite anisotropic crystal has been derived by Eshelby, Read, and Shockley⁽¹⁾ and extended by Foreman⁽²⁾ and by Stroh⁽³⁾. This general method yields results in the form of a sum of terms of complex (in the sense of $\sqrt{-1}$) quantities plus their complex conjugates. The first objective of this work is to carry out for dislocations in the basal plane of graphite the elementary but tedious rationalization of these expressions to obtain formulas containing real quantities only. The results, presented in Section 2, are applicable to dislocations in the basal plane of a hexagonal crystal and for dislocations in certain directions in other crystal systems. In Section 3, formulas previously given in the literature for the line energy of dislocations in symmetry directions are expressed in terms of the notation used in this report. Numerical results are given for these dislocations in graphite and several metals.

The second objective of this work is to use the stress components for the anisotropic case to calculate by standard methods the dependence of stacking fault energy on width of an extended dislocation, on width of a triple partial ribbon, and on radius of curvature of an extended node. These formulas and a tractable formula for the force between parallel dislocations in the orientations mentioned above are presented in Section 4. Experimental values reported by electron microscopists of dislocation widths and radii of curvature in graphite have been used to obtain an estimate of the stacking fault energy of graphite.

The thickness of films used in electron microscopy is of the order of 1000 Å, which is about the same as the width of an extended dislocation in graphite. Since the distance between partial dislocations is comparable to the distance from the partials to the surface, it appears to be possible that the stress-free surfaces of the film might considerably affect the width of an extended dislocation. The third objective of this work is to calculate the variation in width of an extended dislocation lying parallel to a plane, stress-free surface as a function of distance of the dislocation from the surface. In Section 5 results are given for an arbitrarily oriented dislocation in an isotropic solid with a plane surface and for a 30° extended dislocation and a symmetrical, screw triple partial ribbon in an anisotropic plate. The results are applied to graphite.

Manuscript released by author April 1962 for publication as an ASD Technical Documentary Report.

The work reported herein forms a part of a broad and long range investigation of the theory of the mechanical properties of graphite. In anticipation of future needs, all the stress and displacement components have been obtained, although only a few stress components were needed for the specific applications mentioned above.

In some instances the application of dislocation theory to the mechanical properties of graphite is the same as that for metals. Consequently, it is occasionally desirable to compare a result for graphite with the corresponding result for metals, particularly the close-packed metals. In order to do this, the notation used in this work has been kept general, and certain results applicable to metals but not to graphite have been obtained. This was necessary, for example, in order to evaluate the effect of neglecting the Peierls force by comparing the relation between stacking fault energy and dislocation width derived here with other work in the literature on certain hexagonal close-packed and face-centered cubic metals.

The main results are summarized in Section 6.

2. DISLOCATIONS IN SYMMETRY DIRECTIONS

The formulas of the general theory for the components of displacement and stress of a dislocation consist of a sum of products of complex numbers. Their simple analytical form makes these formulas useful for general theoretical applications; but the explicit dependence on the elastic constants and on the coordinates is obscured by the complex number formalism. For certain orientations of the coordinate system the final results can be expressed in terms of real quantities in a way that is only slightly more complicated than the corresponding formulas for an isotropic medium. The explicit dependence on the elastic constants is also easily surveyed. In the first section the conditions on the elastic constants are derived under which the general theory simplifies. Next, the displacement and stress components and certain other related quantities are obtained for dislocations in the special symmetry directions. Finally, the stress and displacement components of a screw dislocation in certain symmetry directions parallel to the surfaces of an anisotropic plate are obtained.

2.1. Derivation of Conditions on the Elastic Constants

Eshelby et al.⁽¹⁾ and others^(2,3,4) have pointed out that the general theory of dislocations in anisotropic crystals becomes much simpler when the dislocations are along certain directions of high crystal symmetry. The usual method of deriving the conditions under which the theory simplifies is to require the vanishing of certain coefficients in an algebraic equation (the sixth degree equation for p in Eshelby et al.'s paper). This procedure yields certain restrictions on the elastic constants c_{ij} defined with respect to a set of Cartesian coordinates with x_3 parallel to the i_j direction of the straight, infinitely long dislocation. Under these restrictions on the c_{ij} one then finds that the screw and edge components of the dislocation become completely independent in the sense that the screw component u_3 of the displacement from equilibrium depends

only on the screw component b_3 of the Burgers vector and the edge components of displacement u_1 and u_2 depend only on the edge components b_1 and b_2 of the Burgers vector. The following alternative derivation of the conditions for the separation of edge and screw components may be of some interest in that it is more direct and shows the necessity as well as the sufficiency of the restrictions on the c_{ij} .

The fundamental requirement of the general theory is that the elastic field be independent of x_3 . Under this restriction the three equilibrium conditions on the stresses τ_{jk} reduce to

$$\sum_{k=1}^2 \partial \tau_{jk} / \partial x_k = 0 \quad . \quad (2.1.1)$$

Combining these with the stress-strain relations expressed in terms of derivatives of the displacements u_i yields three simultaneous second-order partial differential equations for the u_i . One way of simplifying these equations is to impose restrictions on the elastic constants which will uncouple one displacement component from the other two. From the stress-strain relations one finds that τ_{12} contains a term $c_{66} (\partial u_1 / \partial x_2 + \partial u_2 / \partial x_1)$. Since c_{66} is always greater than zero, it follows from (2.1.1) that the first two equilibrium equations will always contain u_1 and u_2 . Therefore, the only possibility for uncoupling the displacements is to eliminate u_3 from the first two equilibrium equations and u_1 and u_2 from the third equation. On carrying out the algebra one finds the restrictions $c_{14} = c_{15} = c_{24} = c_{25} = c_{46} = c_{56} = 0$, already noted in the references cited above. For convenience of reference we will refer to a set of elastic constants for which at least these six c_{ij} are zero as Type II constants. This analysis shows that the separation of the elastic field of the dislocation into edge and screw components for Type II constants results from an uncoupling of the fundamental equations of equilibrium and that this uncoupling can be done in only one way.

It has been pointed out by Eshelby (1) and by Foreman (2) that the algebraic manipulations of the general theory for Type II elastic constants become much simpler when the only nonzero constants are c_{11} , c_{12} , c_{13} , c_{22} , c_{23} , c_{33} , c_{44} , c_{55} , and c_{66} . A set of elastic constants for which these are the only nonzero c_{ij} will be denoted as Type I constants. Type I constants are a particularly simple case of Type II constants for which the sixth degree equation for p , referred to above, factors into one equation quadratic in p^2 and one equation quadratic in p . The orientations of the coordinates x_i with respect to crystallographic axes for which the elastic constants are Type I or II are given without derivation in references (1) to (4). In the Appendix we outline a simple derivation of these orientations.

Except for the Appendix, the remaining results of this work apply to Type I elastic constants only.

2.2. Displacements, Stresses, and Related Quantities for Type I Elastic Constants

2.2.1. Definitions of δ_j , C_j , and C_j^*

For Type I elastic constants the formulas of the general theory for the displacements, stresses, and related quantities can be put in a form which does not contain complex numbers and which gives the explicit dependence on the elastic constants. In order to present the final results in a compact form, we introduce the following symbols:

$$\delta_1 = \sqrt{\frac{c_{11}}{c_{22}}}, \quad \delta_2 = \frac{c_{11}c_{22} - c_{12}^2 - 2c_{12}c_{66}}{c_{22}c_{66}}, \quad \delta_3 = \frac{c_{55}}{c_{44}}, \quad (2.2.1)$$

$$\delta_4 = \frac{c_{13}c_{22} - c_{12}c_{23}}{c_{11}c_{22} - c_{12}^2}, \quad \delta_5 = \frac{c_{11}c_{23} - c_{12}c_{13}}{c_{11}c_{22} - c_{12}^2}. \quad (2.2.2)$$

If $2c_{66} = \sqrt{c_{11}c_{22}} - c_{12}$, defined as Case 3 in Section 2.2.2,

$$\delta_2 = 2\delta_1 = 2\sqrt{\frac{c_{11}}{c_{22}}}. \quad (2.2.3)$$

The most important examples of Case 3 are all dislocations in isotropic crystals and dislocations parallel to the c axis in crystals of the hexagonal system. For these examples

$$\delta_1 = 1, \quad \delta_2 = 2, \quad \text{and} \quad \delta_3 = 1; \quad (2.2.4)$$

while for isotropic crystals only

$$\delta_4 = \delta_5 = \frac{c_{12}}{c_{11} + c_{12}} = \nu, \quad (2.2.5)$$

where

$$\nu = \frac{c_{12}}{c_{11} + c_{12}} = \text{Poisson's Ratio}. \quad (2.2.6)$$

The δ_j are dimensionless real parameters that in part characterize the anisotropy of the crystal.

Contrails

Let
$$C_1 = \frac{c_{11} c_{22} - c_{12}^2}{2\pi c_{22} (2\delta_1 + \delta_2)^{1/2}} \quad (2.2.7)$$

$$C_2 = (c_{44} c_{55})^{1/2} / 2\pi \quad (2.2.8)$$

From (2.2.1)

$$2\delta_1 + \delta_2 = (\sqrt{c_{11} c_{22}} - c_{12}) (\sqrt{c_{11} c_{22}} + c_{12} + 2c_{66}) / c_{22} c_{66} \quad (2.2.9)$$

The stability conditions for the elastic stiffness constants are in part that each factor on the right-hand side be positive. Hence

$$2\delta_1 + \delta_2 > 0 \quad , \quad (2.2.10)$$

and C_1 and C_2 are always real positive constants. For Case 3

$$C_1 = (c_{11} c_{22} - c_{12}^2) / 4\pi (c_{11} c_{22})^{1/2} \quad (2.2.11)$$

and for isotropic crystals

$$C_1 = (c_{11}^2 - c_{12}^2) / 4\pi c_{11} = G / 2\pi (1 - \nu) \quad (2.2.12)$$

$$C_2 = (c_{11} - c_{12}) / 4\pi = G / 2\pi \quad , \quad (2.2.13)$$

where

$$G = (c_{11} - c_{12}) / 2 = \text{Shear Modulus.} \quad (2.2.14)$$

The C_j have the dimensions of elastic stiffness constants and for anisotropic material replace the quantities (2.2.12) and (2.2.13) which occur for isotropic material.

Certain formulas obtain their simplest form in terms of the quantities

$$C_1^* = \frac{C_1}{4\delta_1} = (c_{11} c_{22} - c_{12}^2) / 8\pi \delta_1 c_{22} (2\delta_1 + \delta_2)^{1/2} \quad (2.2.15)$$

$$C_2^* = \frac{C_2}{4} = (c_{44} c_{55})^{1/2} / 8\pi \quad . \quad (2.2.16)$$

For Case 3

$$C_1^* = (c_{11} c_{22} - c_{12}^2) / 16\pi c_{11} \quad , \quad (2.2.17)$$

and for isotropic materials

$$C_1^* = (c_{11}^2 - c_{12}^2) / 16\pi c_{11} = G / 8\pi (1 - \nu) \quad (2.2.18)$$

$$C_2^* = (c_{11} - c_{12}) / 16\pi = G / 8\pi \quad (2.2.19)$$

2.2.2. The p_i , A_{ij} , D_i , B_{ij} and d_i

The general theory of dislocations in anisotropic crystals has been given in detail in the papers of Eshelby et al. ⁽¹⁾ and Stroh ⁽³⁾ and for brevity will not be repeated here. The general theory contains a number of quantities defined implicitly as the solutions of certain equations. For nonsymmetry directions of the dislocation line these equations can only be solved numerically, but for Type I elastic constants the explicit, analytical dependence on the elastic constants and components b_i of the Burgers vector can be obtained for the quantities defined by Eshelby et al. and by Stroh. These new results are given below. The inherent arbitrariness in the quantities ¹ A_{ij} and D_i is fixed by using Stroh's choice of his matrix elements L_{ij} . Three cases must be considered; quantities which are different for the three cases are given first, followed by those which are the same for all three cases. Let the subscripts R and I denote the real and imaginary parts of complex numbers and let the index β have the values 1, 2. The following results are only applicable for Type I elastic constants.

Case 1: $2\delta_1 < \delta_2$ or $2c_{66} < (c_{11} c_{22})^{1/2} - c_{12}$

$$p_{\beta R} = 0 \quad p_{\beta I} = 2^{-1/2} \left[\delta_2 - (-1)^\beta (\delta_2^2 - 4\delta_1^2)^{1/2} \right]^{1/2} \quad (2.2.20)$$

$$A_{1\beta I} = 0 \quad A_{1\beta R} = -(c_{22} p_{\beta I}^2 + c_{12}) / (c_{11} c_{22} - c_{12}^2) \quad (2.2.21)$$

$$A_{2\beta R} = 0 \quad A_{2\beta I} = -(c_{12} p_{\beta I}^2 + c_{11}) / (c_{11} c_{22} - c_{12}^2) p_{\beta I} \quad (2.2.22)$$

$$D_{\beta R} = (-1)^\beta (c_{11} c_{22} - c_{12}^2) b_1 / 2c_{22} (\delta_2^2 - 4\delta_1^2)^{1/2} \quad (2.2.23)$$

$$D_{\beta I} = (-1)^\beta (c_{11} c_{22} - c_{12}^2) b_2 / 2c_{22} (\delta_2^2 - 4\delta_1^2)^{1/2} p_{\beta I} \quad (2.2.24)$$

¹ This A_{ij} is equal to the $A_{(j)i}$ of Eshelby et al.

Contrails

Case 2: $2\delta_1 > \delta_2$ or $2c_{66} > (c_{11}c_{22})^{1/2} - c_{12}$

$$p_{\beta R} = (-1)^{\beta-1} 2^{-1} (2\delta_1 - \delta_2)^{1/2} \quad (2.2.25)$$

$$p_{\beta I} = 2^{-1} (2\delta_1 + \delta_2)^{1/2} \quad (2.2.26)$$

$$A_{1\beta R} = -(c_{22}\delta_2 + 2c_{12})/2(c_{11}c_{22} - c_{12}^2) \quad (2.2.27)$$

$$A_{1\beta I} = (-1)^{\beta-1} c_{22} (4\delta_1^2 - \delta_2^2)^{1/2} / 2(c_{11}c_{22} - c_{12}^2) \quad (2.2.28)$$

$$A_{2\beta R} = (-1)^{\beta-1} (c_{22}\delta_1 - c_{12})(2\delta_1 - \delta_2)^{1/2} / 2(c_{11}c_{22} - c_{12}^2) \quad (2.2.29)$$

$$A_{2\beta I} = -(c_{22}\delta_1 + c_{12})(2\delta_1 + \delta_2)^{1/2} / 2(c_{11}c_{22} - c_{12}^2) \quad (2.2.30)$$

$$D_{\beta R} = (-1)^{\beta-1} (c_{11}c_{22} - c_{12}^2) b_2 / 4c_{22}\delta_1 (2\delta_1 - \delta_2)^{1/2} \quad (2.2.31)$$

$$D_{\beta I} = \frac{c_{11}c_{22} - c_{12}^2}{4c_{22}\delta_1 (2\delta_1 + \delta_2)^{1/2}} \left[\frac{(-1)^\beta 2\delta_1 b_1}{(2\delta_1 - \delta_2)^{1/2}} + b_2 \right] \quad (2.2.32)$$

Case 3: $2\delta_1 = \delta_2$ or $2c_{66} = (c_{11}c_{22})^{1/2} - c_{12}$

$$p_{\beta R} = 0, \quad p_{\beta I} = \delta_1^{1/2} \quad (2.2.33)$$

In this case, two of the p_i are equal and the general theory for the other quantities does not apply.

Cases 1, 2, and 3

$$p_{3R} = 0, \quad p_{3I} = \delta_3^{1/2} \quad (2.2.34)$$

$$A_{13} = A_{23} = A_{31} = A_{32} = 0 \quad (2.2.35)$$

$$A_{33R} = 0 \quad A_{33I} = -1/(c_{44}c_{55})^{1/2} \quad (2.2.36)$$

Contrails

$$D_{3R} = 0 \quad D_{3I} = (c_{44}c_{55})^{1/2} b_3/2 \quad (2.2.37)$$

$$[B_{jk}] = \frac{1}{2\pi} \begin{bmatrix} C_1^{-1} & 0 & 0 \\ 0 & \delta_1 C_1^{-1} & 0 \\ 0 & 0 & C_2^{-1} \end{bmatrix} \quad (2.2.38)$$

$$d_1 = 2\pi C_1 b_1 \quad d_2 = 2\pi \delta_1^{-1} C_1 b_2 \quad d_3 = 2\pi C_2 b_3 \quad (2.2.39)$$

Stroh's matrix elements L_{ij} and M_{ij} are functions of the p_i . The expressions for the real and imaginary parts of these matrix elements can be obtained so easily from Stroh's formulas and the formulas above for the p_i that the results need not be given here.

2.2.3. The Displacements u_i

Outside the core of a dislocation the leading terms in the series expansions of the components u_i of the elastic displacements from equilibrium, due to a dislocation along the x_3 axis, can be expressed in terms of real quantities in the following way:

$$u_i = (2\pi)^{-1} \sum_j \left\{ (A_{ijR} D_{jI} + A_{ijI} D_{jR}) \ln[x_1^2 + 2p_{jR} x_1 x_2 + (p_{jR}^2 + p_{jI}^2)x_2^2] \right. \\ \left. + 2(A_{ijR} D_{jR} - A_{ijI} D_{jI}) \tan^{-1}[p_{jI} x_2 / (x_1 + p_{jR} x_2)] \right\} + u_{0i} \quad (2.2.40)$$

in which i, j take the values 1, 2, 3. The constants u_{0i} represent a uniform translation of the entire lattice and are usually chosen to make the logarithmic terms vanish at atomic distances and to locate the slip plane across which the u_i are discontinuous.

Although formulas (2.2.40) in conjunction with the results given above are suitable for numerical computations, they do not readily reveal the dependence of the u_i on the elastic constants and Burgers vector. On substituting the expressions given by (2.2.20) to (2.2.37) into (2.2.40), one obtains the following results.

Contrails

Case 1

$$u_1 = \sum_{\alpha=1}^2 (-1)^{\alpha-1} \frac{c_{22} p_{\alpha I}^2 + c_{12}}{4\pi c_{22} (\delta_2^2 - 4\delta_1^2)^{1/2}} \left[\frac{b_2}{p_{\alpha I}} \ln(x_1^2 + p_{\alpha I}^2 x_2^2) + 2b_1 \tan^{-1} p_{\alpha I} x_2/x_1 \right] + u_{01} \quad (2.2.41)$$

$$u_2 = \sum_{\alpha=1}^2 (-1)^{\alpha-1} \frac{c_{12} p_{\alpha I}^2 + c_{11}}{4\pi c_{22} (\delta_2^2 - 4\delta_1^2)^{1/2} p_{\alpha I}} \left[b_1 \ln(x_1^2 + p_{\alpha I}^2 x_2^2) - \frac{2b_2}{p_{\alpha I}} \tan^{-1} p_{\alpha I} x_2/x_1 \right] + u_{02} \quad (2.2.42)$$

Case 2

$$u_1 = \sum_{\alpha=1}^2 \left\{ \left[(-1)^{\alpha-1} \frac{c_{11}c_{22} - c_{12}^2}{8\pi c_{22}c_{66} (4\delta_1^2 - \delta_2^2)^{1/2}} b_1 + \frac{(c_{11}c_{22})^{1/2} - c_{12}}{8\pi [c_{11}c_{22} (2\delta_1 + \delta_2)]^{1/2}} b_2 \right] \right. \\ \left. \ln[x_1^2 - (-1)^\alpha (2\delta_1 - \delta_2)^{1/2} x_1 x_2 + \delta_1 x_2^2] + \left[\frac{b_1}{4\pi} \right. \right. \\ \left. \left. + (-1)^\alpha \frac{(c_{11}c_{22})^{1/2} + c_{12}}{4\pi [c_{11}c_{22} (2\delta_1 - \delta_2)]^{1/2}} b_2 \right] \tan^{-1} \frac{(2\delta_1 + \delta_2)^{1/2} x_2}{2x_1 - (-1)^\alpha (2\delta_1 - \delta_2)^{1/2} x_2} \right\} + u_{01} \quad (2.2.43)$$

$$u_2 = \sum_{\alpha=1}^2 \left\{ \left[-\frac{(c_{11}c_{22})^{1/2} - c_{12}}{8\pi c_{22} (2\delta_1 + \delta_2)^{1/2}} b_1 + (-1)^\alpha \frac{c_{11}c_{22} - c_{12}^2}{8\pi c_{22}c_{66} (4\delta_1^2 - \delta_2^2)^{1/2}} b_2 \right] \right. \\ \left. \ln[x_1^2 - (-1)^\alpha (2\delta_1 - \delta_2)^{1/2} x_1 x_2 + \delta_1 x_2^2] + \left[(-1)^\alpha \frac{(c_{11}c_{22})^{1/2} + c_{12}}{4\pi c_{22} (2\delta_1 - \delta_2)^{1/2}} b_1 \right. \right. \\ \left. \left. + \frac{b_2}{4\pi} \right] \tan^{-1} \frac{(2\delta_1 + \delta_2)^{1/2} x_2}{2x_1 - (-1)^\alpha (2\delta_1 - \delta_2)^{1/2} x_2} \right\} + u_{02} \quad (2.2.44)$$

The formulas for Case 3 can be obtained from those of either Case 1 or Case 2 by a limiting procedure in which δ_2 approaches $2\delta_1$.

$$\begin{aligned}
 \text{Case 3} \\
 u_1 = \frac{b_2}{4\pi(\delta_1)^{1/2}} \left[\frac{(c_{11}c_{22})^{1/2} - c_{12}}{2(c_{11}c_{22})^{1/2}} \ln(x_1^2 + \delta_1 x_2^2) + \frac{(c_{11}c_{22})^{1/2} + c_{12}}{c_{22}} \frac{x_2^2}{x_1^2 + \delta_1 x_2^2} \right] \\
 + \frac{b_1}{2\pi} \left[\tan^{-1} \frac{(\delta_1)^{1/2} x_2}{x_1} + \frac{[(c_{11}c_{22})^{1/2} + c_{12}] \delta_1^{1/2}}{2(c_{11}c_{22})^{1/2}} \frac{x_1 x_2}{x_1^2 + \delta_1 x_2^2} \right] + u_{01} \quad (2.2.45)
 \end{aligned}$$

$$\begin{aligned}
 u_2 = \frac{b_1(\delta_1)^{1/2}}{4\pi} \left[-\frac{(c_{11}c_{22})^{1/2} - c_{12}}{2(c_{11}c_{22})^{1/2}} \ln(x_1^2 + \delta_1 x_2^2) + \frac{(c_{11}c_{22})^{1/2} + c_{12}}{c_{22}} \frac{x_2^2}{x_1^2 + \delta_1 x_2^2} \right] \\
 + \frac{b_2}{2\pi} \left[\tan^{-1} \frac{(\delta_1)^{1/2} x_2}{x_1} - \frac{[(c_{11}c_{22})^{1/2} + c_{12}] \delta_1^{1/2}}{2(c_{11}c_{22})^{1/2}} \frac{x_1 x_2}{x_1^2 + \delta_1 x_2^2} \right] + u_{02} \quad (2.2.46)
 \end{aligned}$$

In most applications of Case 3, $c_{11} = c_{22}$ and $\delta_1 = 1$, which considerably simplifies (2.2.45) and (2.2.46).

Cases 1, 2, and 3

$$u_3 = (b_3/2\pi) \tan^{-1} \delta_3^{1/2} x_2/x_1 + u_{03} \quad (2.2.47)$$

In order to get the well-known formulas for isotropic materials, set $\delta_1 = \delta_3 = 1$ and note that

$$\frac{2x_2^2}{x_1^2 + x_2^2} = 1 - \frac{x_1^2 - x_2^2}{x_1^2 + x_2^2} \quad (2.2.48)$$

2.2.4. The Stresses τ_{ij}

Unlike the displacements, the general formulas for the stress components of a dislocation along the x_3 axis simplify considerably on substituting into the general formulas the values of the A_{ij} , D_j , and p_j given by (2.2.20) to (2.2.37). Furthermore, the results are valid for all three cases.

Cases 1, 2, and 3

$$\tau_{11} = C_1 \frac{-b_1 x_2 [(\delta_1 + \delta_2)x_1^2 + \delta_1^2 x_2^2] + b_2 x_1 (x_1^2 - \delta_1 x_2^2)}{x_1^4 + \delta_2 x_1^2 x_2^2 + \delta_1^2 x_2^4} \quad (2.2.49)$$

$$\tau_{12} = C_1 \frac{(b_1 x_1 + b_2 x_2) (x_1^2 - \delta_1 x_2^2)}{x_1^4 + \delta_2 x_1^2 x_2^2 + \delta_1^2 x_2^4} \quad (2.2.50)$$

$$\tau_{22} = C_1 \frac{b_1 x_2 (x_1^2 - \delta_1 x_2^2) + b_2 x_1 [\delta_1^{-1} x_1^2 + (1 + \delta_2/\delta_1) x_2^2]}{x_1^4 + \delta_2 x_1^2 x_2^2 + \delta_1^2 x_2^4} \quad (2.2.51)$$

$$\tau_{13} = -C_2 \frac{b_3 \delta_3 x_2}{x_1^2 + \delta_3 x_2^2} \quad (2.2.52)$$

$$\tau_{23} = C_2 \frac{b_3 x_1}{x_1^2 + \delta_3 x_2^2} \quad (2.2.53)$$

$$\tau_{33} = \delta_4 \tau_{11} + \delta_5 \tau_{22} \quad (2.2.54)$$

In the usual applications of Case 3, one has $2\delta_1 = \delta_2 = 2\delta_3 = 2$ and these formulas reduce to the same functional form as the well-known stress components in an isotropic material.

2.3. Screw Dislocation in an Anisotropic Flat Plate

For later applications we shall need the stress components of a straight screw dislocation lying parallel to the stress-free surfaces of a flat plate of infinite lateral extent. Let d be the thickness of the plate and a be the distance of the dislocation line from one of the free surfaces. The coordinate system is chosen as shown in Figure 1. The stress and displacement components of a dislocation in an infinite medium must be modified to make the stresses satisfy the boundary conditions,

$$\left. \begin{aligned} \tau_{11} = 0, \quad \tau_{12} = 0, \quad \tau_{13} = 0 \\ \text{at } x_1 = 0 \text{ and } x_1 = -d \end{aligned} \right\} 2.3.1$$

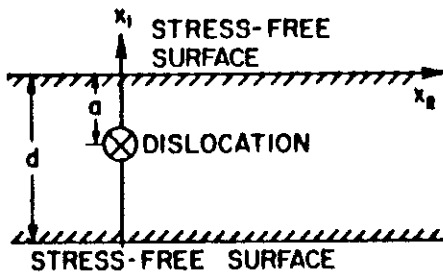


Figure 1. Coordinate system for a dislocation in a flat plate.

that the surfaces of the flat plate be stress free. Leibfried and Dietze ⁽⁵⁾ have solved the corresponding problem of a screw dislocation in a flat plate of isotropic material. Their method was to add infinite sequences of "image" screw dislocations above and below the plate. This method can also be applied to the case of a flat plate of an anisotropic crystal. We assume as always that the orientation is such that the elastic constants are of Type I.

2.3.1. The Stress Components

For a screw dislocation the only nonvanishing stress components are τ_{13} and τ_{23} . If the dislocation line passes through the point $(-a, 0, 0)$, then by (2.2.52) and (2.2.53) these components in an infinite crystal are

$$\tau_{13}^{\infty} = -C_2 \frac{b_3 \delta_3 x_2}{(x_1 + a)^2 + \delta_3 x_2^2} \quad (2.3.2)$$

and

$$\tau_{23}^{\infty} = C_2 \frac{b_3 (x_1 + a)}{(x_1 + a)^2 + \delta_3 x_2^2} \quad (2.3.3)$$

Leibfried and Dietze show that the surfaces can be made stress free by adding infinite sequences of "image" dislocations along the positive and negative x_1 axis. Using the same procedure for the case of Type I elastic constants, we obtain

$$\tau_{13} = \delta_3 C_2 b_3 x_2 \sum_{n=-\infty}^{\infty} \left[\frac{1}{(x_1 - a + 2nd)^2 + \delta_3 x_2^2} - \frac{1}{(x_1 + a + 2nd)^2 + \delta_3 x_2^2} \right] \quad (2.3.4)$$

and

$$\tau_{23} = C_2 b_3 \sum_{n=-\infty}^{\infty} \left[\frac{x_1 + a + 2nd}{(x_1 + a + 2nd)^2 + \delta_3 x_2^2} - \frac{x_1 - a + 2nd}{(x_1 - a + 2nd)^2 + \delta_3 x_2^2} \right] \quad (2.3.5)$$

Summing these by the method of Leibfried and Dietze, we obtain

$$\tau_{13} = \frac{\pi \delta_3^{1/2} C_2 b_3}{2d} \left[\frac{\sinh \pi \delta_3^{1/2} d^{-1} x_2}{\cosh \pi \delta_3^{1/2} d^{-1} x_2 - \cos \pi d^{-1} (x_1 - a)} - \frac{\sinh \pi \delta_3^{1/2} d^{-1} x_2}{\cosh \pi \delta_3^{1/2} d^{-1} x_2 - \cos \pi d^{-1} (x_1 + a)} \right] \quad (2.3.6)$$

and

$$\tau_{23} = \frac{\pi C_2 b_3}{2d} \left[\frac{\sin \pi d^{-1} (x_1 + a)}{\cosh \pi \delta_3^{1/2} d^{-1} x_2 - \cos \pi d^{-1} (x_1 + a)} - \frac{\sin \pi d^{-1} (x_1 - a)}{\cosh \pi \delta_3^{1/2} d^{-1} x_2 - \cos \pi d^{-1} (x_1 - a)} \right] \quad (2.3.7)$$

It can directly be verified that these expressions satisfy the equations of equilibrium and the boundary conditions and represent a dislocation through the point $(-a, 0, 0)$. Unfortunately, this method cannot be used to find the stress components of an edge dislocation in a thin plate.

2.3.2. The Displacements

The only nonzero displacement, u_3 , can be found by the same method used to obtain the stress components. There results

$$u_3 = \frac{b_3}{2\pi} \sum_{n=-\infty}^{\infty} \left[\tan^{-1} \frac{\delta_3^{1/2} x_2}{x_1 + a + 2nd} - \tan^{-1} \frac{\delta_3^{1/2} x_2}{x_1 - a + 2nd} \right] + u_{03} \quad (2.3.8)$$

As suggested by Leibfried and Dietze, we integrate (2.3.6) and (2.3.7), rather than sum (2.3.8), to obtain

$$u_3 = \frac{b_3}{2\pi} \left[\tan^{-1} \frac{\tanh \pi \delta_3^{1/2} x_2 / 2d}{\tan \pi (x_1 + a) / 2d} - \tan^{-1} \frac{\tanh \pi \delta_3^{1/2} x_2 / 2d}{\tan \pi (x_1 - a) / 2d} \right] + u_{03} \quad (2.3.9)$$

This applies only to Type I elastic constants.

3. LINE ENERGY OF DISLOCATIONS

In this section some results pertaining to the line energy of a dislocation which have been previously given in the literature are reformulated in terms of the present notation. It is shown that as a consequence of the near-isotropic nature of a (111) plane in a FCC crystal a simple formula for the line energy of dislocations along face diagonals is approximately valid for dislocations in arbitrary orientations in (111) planes. This result is important for the estimation of stacking fault energies. Numerical results are given for the line energies of dislocations in symmetry directions in cubic and hexagonal crystals.

3.1. Analytical Results

The formula for the elastic energy per unit length of the stress field of a straight dislocation contained within a cylinder of outer radius R and inner radius r_0 was first obtained for Type I elastic constants by Foreman⁽²⁾ by another method. The formula is also obtained easily from Stroh's formula(56) in reference (3) and the results (2.2.38) and (2.2.39) given in the preceding section. For convenience of reference this formula for the elastic energy per unit length is given here in terms of the present notation. For Type I elastic constants

$$U = \frac{1}{2} [C_1 b_1^2 + (C_1 / \delta_1) b_2^2 + C_2 b_3^2] \ln R / r_0 \quad (3.1.1)$$

For most dislocations of interest in cubic and hexagonal crystals this formula can be put in the form¹

$$U = K b^2 \ln R / r_0 \quad (3.1.2)$$

¹ This K is equal to the $K/4\pi$ of Foreman⁽²⁾ and DeWit and Koehler⁽⁶⁾.

Contrails

in which b is the magnitude of the Burgers vector and

$$K = \frac{1}{2} [K_{\text{screw}} + K_{\text{edge}} + (K_{\text{screw}} - K_{\text{edge}}) \cos 2\alpha] \quad , \quad (3.1.3)$$

where α is the angle between the Burgers vector and the dislocation line. The explicit form of K_{screw} and K_{edge} for the common possible slip planes (the plane containing the Burgers vector and dislocation line) is given in Table 1.

TABLE 1
ANALYTICAL LINE ENERGY FACTORS FOR DISLOCATIONS

| Dislocation Direction | Slip Plane | K_{screw} | K_{edge} | Formula for c_{ij} |
|---------------------------|------------|--------------------|----------------------------|----------------------|
| <u>Hexagonal Crystals</u> | | | | |
| Basal | Basal | $2C_2^*$ | $2C_1^*$ | I. 2. 2 |
| | Prismatic | $2C_2^*$ | $\frac{1}{2} C_1$ | I. 2. 2 |
| C Axis | Prismatic | $2C_2^*$ | $2C_1^*$ | I. 2. 1 |
| <u>Cubic Crystals</u> | | | | |
| < 001 > | (hk 0) | $2C_2^*$ | $2C_1^*$ | I. 2. 3 |
| < 110 > | (001) | $2C_2^*$ | $2C_1^*$ | I. 2. 4 |
| | (110) | $2C_2^*$ | $\frac{1}{2} C_1$ | I. 2. 4 |
| | (111) | $2C_2^*$ | $2C_1^* (1 + 2\delta_1)/3$ | I. 2. 4 |

The last column in the table indicates the formula in Appendix I which gives the elastic constants with respect to the dislocation coordinate axes in terms of the standard tabulated elastic constants. The K for dislocations other than screw or edge are easily found from (3.1.3). For example, for a 30° partial dislocation in the <110> direction in the (111) slip plane $K = \frac{1}{4} (3K_{\text{screw}} + K_{\text{edge}}) = \frac{1}{2} [C_1^* (1 + 2\delta_1) 3^{-1} + 3C_2^*]$.

3.2. Numerical Results

The numerical values of the energy factors K_{screw} and K_{edge} are given in Table 2 for several substances of hexagonal and cubic symmetry for the

TABLE 2
NUMERICAL LINE ENERGY FACTORS FOR DISLOCATIONS

| Substance | Dislocation in Basal Plane | | | Dislocation along c Axis | | |
|---------------------------------------|---|---|---|---|---|---|
| | K_{screw} | K_{edge}, \vec{b} in Basal Plane | K_{edge}, \vec{b} along $\langle 0001 \rangle$ | K_{screw} | K_{edge} | |
| <u>Hexagonal Crystals¹</u> | | | | | | |
| Graphite | 0.25 | 0.36 | 0.072 | 0.018 | 4.3 | |
| Be | 1.17 | 1.23 | 1.32 | 1.29 | 1.15 | |
| Cd | .220 | .282 | .188 | .161 | .404 | |
| Co | .583 | .992 | 1.072 | .601 | .869 | |
| Mg | .131 | .195 | .199 | .130 | .191 | |
| Zn | .395 | .442 | .275 | .309 | .619 | |
| TiB ₂ | 1.49 | 2.14 | 1.71 | 1.99 | 1.78 | |
| Substance | Dislocation along $\langle 001 \rangle$ | | Dislocation along $\langle \bar{1}10 \rangle$ | | | |
| | K_{screw} | K_{edge}, \vec{b} in (hk0) Plane | K_{screw} | K_{edge}, \vec{b} in (001) Plane | K_{edge}, \vec{b} in (110) Plane | K_{edge}, \vec{b} in (111) Plane |
| <u>Cubic Crystals¹</u> | | | | | | |
| Ag | 0.367 | 0.332 | 0.211 | 0.420 | 0.376 | 0.391 |
| Al | .225 | .312 | .204 | .324 | .316 | .319 |
| Au | .334 | .342 | .198 | .421 | .394 | .403 |
| Cu | .598 | .502 | .333 | .652 | .570 | .597 |
| Ni | .979 | .873 | .615 | 1.077 | .946 | .990 |
| Pb | .115 | .096 | .058 | .130 | .117 | .121 |
| TiC | 1.39 | 1.83 | 1.46 | 1.79 | 1.82 | 1.81 |

¹ Based on elastic constants given in Table 5 . K in units of 10^{11} dynes/cm².

elastic stiffness constants given in Table 5 (Appendix I). The accuracy of the results depends on the accuracy with which the elastic constants are known. The values for Ag, Al, Au, Cu, and Mg are probably within ± 1 per cent; and the remainder within ± 5 to 10 per cent, except for Be, graphite, and TiB₂. The values of the elastic constants of graphite are at present obtained by indirect means whose accuracy is difficult to evaluate, but ± 25 per cent seems reasonable.

3.2.1. Graphite

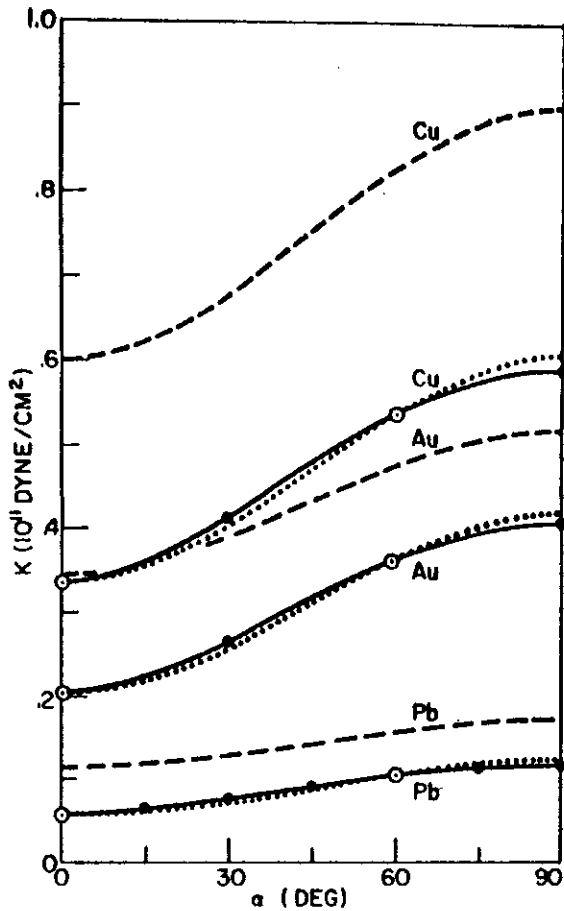
The results for graphite are consistent with a model of elastically rigid planes relatively weakly bound together. For convenience of reference we shall use the following notation due to Fujita and Izui⁽⁷⁾. An edge dislocation in the direction of the c axis is designated as Type 1, a screw dislocation along the c axis as Type 2, a dislocation with a basal slip plane as Type 3, and an edge dislocation in the basal plane with Burgers vector perpendicular to the basal plane (prismatic slip plane) as Type 4. The relative abundance of each type is determined by the core energy, the elastic field energy, the Peierls stress to move the dislocation in the crystal, and the nature of the sources.

Type 3 dislocations should have the lowest core energy and Peierls stress because no C-C bonds in the layer planes are broken for this type. This is confirmed by the fact that Type 3 dislocations are by far the most common type observed by electron microscopy even though their elastic field energy U is roughly twice as great as that of Type 2 dislocations. Type 2 dislocations can be produced by a spiral growth mechanism and have been observed by Tsuzuku⁽⁸⁾. Type 4 dislocations, possibly in conjunction with the easily produced Type 3, also are produced by growth mechanisms either at the edge of extra layer half planes, as observed by Fujita and Izui⁽⁷⁾, or at condensed vacancy disks, as observed by Amelinckx and Delavignette⁽⁹⁾. It is not known at present whether Types 2 and 4 dislocations can be moved in the crystal by external stresses. Since for a Type 1 dislocation the Peierls stress and both the core and elastic field energy are high and the probability of formation by growth is small, this type of dislocation should be very rare; and in fact, it has not been definitely identified experimentally.

3.2.2. Metals

At the present time there is some interest in estimating stacking fault energies in face-centered cubic metals from the radius of curvature of extended dislocation nodes observed by thin-film electron microscopy. The formula, discussed more fully in Section 4.4, relating these quantities contains the line energy of the dislocation. The problem of practical interest is that of the line energy of a partial dislocation arbitrarily oriented with respect to its fixed Burgers vector; on the other hand, formula (3.1.2) solves the problem of a dislocation line fixed in a certain direction with an arbitrarily oriented Burgers vector. For an isotropic material and for dislocations with basal glide planes in hexagonal crystals the two problems are equivalent and have the same solution. Because of the pseudo-isotropic nature of a $\{111\}$ plane in a cubic crystal, the two problems should have almost equal solutions for dislocations with $\{111\}$ glide planes.

Figure 2 shows the variation in K for the two problems of fixed Burgers vector and of fixed dislocation line D as the angle α between \underline{b} and D is varied. The solid curves are for a fixed Burgers vector in the $\langle \bar{1}10 \rangle$ direction and a variable orientation of the dislocation line in the $\{111\}$ plane. The solid curve for gold was computed numerically by Foreman⁽²⁾, that for lead by DeWit⁽⁶⁾,



N-2253

Figure 2. Variation of line energy factor K with angle α between dislocation and Burgers vector for (111) slip plane.

and that for copper both by Foreman and by DeWit. The dotted curve is for a dislocation line in the $\langle 110 \rangle$ direction and different Burgers vectors in the (111) plane. Total dislocations occur at $\alpha = 0^\circ$ and 60° , and partial dislocations at $\alpha = 30^\circ$ and 90° . The dotted and solid curves must coincide at the encircled points. The dashed curves are for an isotropic material with a shear modulus equal to c_{44} and Poisson's ratio of $1/3$. The dotted and isotropic curves were computed for the same elastic constants used by Foreman and DeWit. The maximum difference between the dotted and solid curves is less than 4 per cent; which is probably less than the error in U caused by neglecting the variation in core energy with orientation. The considerable improvement over the values given by isotropic theory is apparent.

Physically, the near isotropic nature of the (111) plane is indicated by the invariance of the velocity of the longitudinal and both transverse sound waves as the direction of propagation in a (111) plane is rotated about an axis perpendicular to that plane. Mathematically, the near isotropy follows from the behavior of the elastic constants with respect to a coordinate system with x_1 in, say, the $\langle 11 \rangle$ direction as x_2 and x_3 are rotated in the (111) plane about x_1 . It can be shown that the only elastic constants which vary are the off-diagonal coupling constants c_{25} , c_{26} , c_{35} , c_{36} ,

c_{45} , and c_{46} . We would not expect the elastic energy to depend strongly on these constants, and in addition, these constants are numerically small (typically, $1/5$) compared to c_{11} . Therefore the curves of K versus α for fixed b and for fixed D should never vary by more than a few per cent.

Several substances have been included in Table 2 only for purposes of comparison. It is seen that only in graphite is there any large variation in K ; and that the elastic line energy of dislocations with basal slip plane in graphite is comparable to that for similar dislocations in Cd and Zn.

4. FORCE BETWEEN DISLOCATIONS AND STACKING FAULT ENERGY

In this section we obtain the specialized form of the formula for the force of interaction between two parallel partial dislocations in an infinite crystal for which the elastic constants are of Type I. These are used to derive the relations between stacking fault energy and widths of extended dislocations and widths of triple partial ribbons. Finally, the relation between stacking fault energy and radius of curvature of an extended node is obtained.

4.1. Force Between Two Parallel Dislocations

Peach and Koehler's ⁽¹⁰⁾ formula for the force per unit length on a dislocation due to its interaction with an external stress field τ_{ij} is

$$\vec{f} = (\vec{b} \cdot \tau) \times \vec{v} \quad , \quad (4.1.1)$$

where \vec{v} is a unit vector in the direction of the dislocation segment.

4.1.1. Arbitrary Burgers Vector and Position

Consider two parallel dislocations D and D' with D along the x_3 axis and D' passing through the point $(x_1, x_2, 0)$. Let \vec{b} be the Burgers vector of D and \vec{b}' that of D'. According to (4.1.1) the components of the force per unit length on D' due to its interaction with D are

$$f_1' = \sum_{i=1}^3 \tau_{zi} b_i', \quad f_2' = - \sum_{i=1}^3 \tau_{ii} b_i', \quad \text{and } f_3' = 0 \quad , \quad (4.1.2)$$

in which τ_{ij} are the stress components of D. Substituting (2.2.49) to (2.2.53) for the τ_{ij} we get for Type I elastic constants,

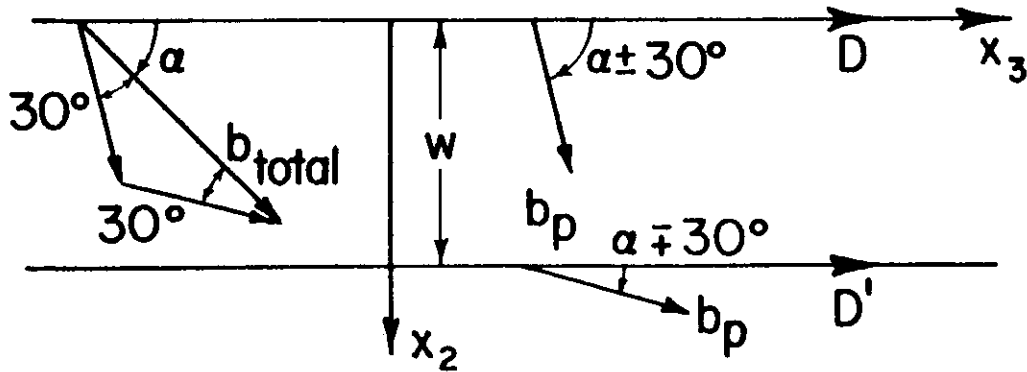
$$f_1' = C_1 \frac{[b_1 b_1' x_1 + (b_1 b_2' + b_2 b_1') x_2] (x_1^2 - \delta_1 x_2^2) + b_2 b_2' x_1 [\delta_1^{-1} x_1^2 + (1 + \delta_2 / \delta_1) x_2^2]}{x_1^4 + \delta_2 x_1^2 x_2^2 + \delta_1^2 x_2^4} + C_2 \frac{b_3 b_3' x_1}{x_1^2 + \delta_3 x_2^2} \quad (4.1.3)$$

and

$$f_2' = C_1 \frac{[(b_1 b_2' + b_2 b_1') x_1 + b_2 b_2' x_2] (-x_1^2 + \delta_1 x_2^2) + b_1 b_1' x_2 [(\delta_1 + \delta_2) x_1^2 + \delta_1^2 x_2^2]}{x_1^4 + \delta_2 x_1^2 x_2^2 + \delta_1^2 x_2^4} + C_2 \frac{b_3 b_3' \delta_3 x_2}{x_1^2 + \delta_3 x_2^2} \quad . \quad (4.1.4)$$

4.1.2. Partial Dislocations in Hexagonal Crystals

Consider a straight, extended dislocation in the basal plane of a hexagonal crystal. If the x_1 axis is taken to be perpendicular to the basal plane, then the elastic constants are of Type I. Let α be the angle between the total Burgers vector and the dislocation line and b_p be the magnitude of the Burgers vector of a partial dislocation, as indicated in Figure 3. If a is



N-1568

Figure 3. Schematic drawing of an extended dislocation in the $x_2 x_3$ plane.

the length of the fundamental lattice vector in the basal plane, then $b_p = a/\sqrt{3}$. From (4.1.2), (4.1.3), and (4.1.4) we find, for the components of the force per unit length on D' due to its interaction with D at a separation w , $f_1' = 0$, $f_3' = 0$, and

$$f_2' = b_p^2 [C_2^* + C_1^* + 2(C_2^* - C_1^*) \cos 2\alpha] w^{-1} \quad (4.1.5)$$

The c_{ij} to be used are expressed in terms of the standard, tabulated elastic constants by formula (I.2.2).

4.1.3. Partial Dislocations in FCC Crystals

Consider a straight, extended dislocation in the $\langle \bar{1}10 \rangle$ direction in a face-centered cubic crystal. If the x_1 axis is taken in the $\langle 001 \rangle$ direction and the x_2 axis in the $\langle 110 \rangle$ direction, then the elastic constants are of Type I. Let α be the angle between the dislocation line and the total Burgers vector in the (111) slip plane. If a is the length of the fundamental lattice vector along a cube edge, then the magnitude of the Burgers vector of a partial dislocation is $b_p = a/\sqrt{6}$. From Figure 4 we see that the partial dislocation D' passes through the point

$$x_1 = -\sqrt{2/3} w, \quad x_2 = w/\sqrt{3}, \quad x_3 = 0 \quad (4.1.6)$$

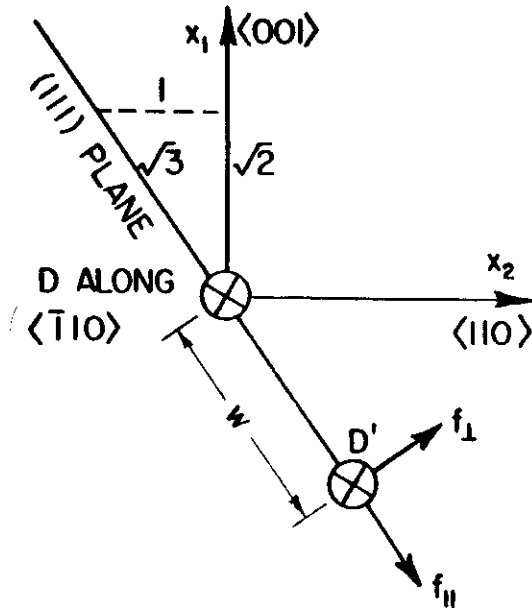


Figure 4. Orientation of an Extended Dislocation in the (111) Plane.

The components of the Burgers vectors of D and D' are

$$\left. \begin{aligned} b_1 &= -\sqrt{2/3} b_p \sin(\alpha \pm 30^\circ) & b_1' &= -\sqrt{2/3} b_p \sin(\alpha \mp 30^\circ) \\ b_2 &= (b_p/\sqrt{3}) \sin(\alpha \pm 30^\circ) & b_2' &= (b_p/\sqrt{3}) \sin(\alpha \mp 30^\circ) \\ b_3 &= b_p \cos(\alpha \pm 30^\circ) & b_3' &= b_p \cos(\alpha \mp 30^\circ) \end{aligned} \right\} (4.1.7)$$

Substitution of these into (4.1.3) and (4.1.4) gives, for the nonzero components of the force per unit length on D' due to its interaction with D,

$$f_1' = -\sqrt{\frac{2}{3}} \frac{b_p^2}{w} \left[C_1^* \frac{2+9\delta_1-4\delta_1^2+\delta_2}{4+\delta_1^2+2\delta_2} (1-2\cos 2\alpha) + C_2^* \frac{3}{2+\delta_3} (1+2\cos 2\alpha) \right] \quad (4.1.8)$$

and

$$f_2' = \frac{b_p^2}{\sqrt{3} w} \left[C_1^* \frac{\delta_1(-10+9\delta_1+2\delta_1^2+4\delta_2)}{4+\delta_1^2+2\delta_2} (1-2\cos 2\alpha) + C_2^* \frac{3\delta_1}{2+\delta_3} (1+2\cos 2\alpha) \right] \quad (4.1.9)$$

From these we obtain the component f_{11}' in the (111) plane and the component $f_{1\perp}'$ perpendicular to the (111) plane:

$$f_{11}' = \frac{b_p^2}{w} \left[C_2^* + C_1^* \frac{1+2\delta_1}{3} + 2 \left(C_2^* - C_1^* \frac{1+2\delta_1}{3} \right) \cos 2\alpha \right] \quad (4.1.10)$$

and

$$f_{11}' = \frac{\sqrt{2} b_p^2}{w} \left[-C_1^* \frac{2+19\delta_1-13\delta_1^2-2\delta_1^3-4\delta_1\delta_2+\delta_2}{3(4+\delta_1^2+2\delta_2)} (1-2\cos 2\alpha) + C_2^* \frac{\delta_3-1}{2+\delta_3} (1+2\cos 2\alpha) \right], \quad (4.1.11)$$

in which f_{11}' and w are positive in the $\langle 11\bar{2} \rangle$ direction and f_{11}' is positive in the $\langle 111 \rangle$ direction. The c_{ij} to be used are expressed in terms of the standard, tabulated elastic constants by formula (I.2.4). Note that, unlike the situation in isotropic and hexagonal crystals, there is now a force f_{11}' which tends to make a partial dislocation climb out of the (111) slip plane.

4.1.4. Dislocations with Equal Burgers Vector

Consider two straight parallel dislocations (partial or complete) with a common slip plane and equal Burgers vectors. We assume that the elastic constants are of Type I for the coordinates shown in Figure 5. Let α be the angle between the Burgers vector and the dislocation line, b be the magnitude of the Burgers vector, and w be the distance between dislocations. From (4.1.2) to (4.1.4) we find, for the components of the force per unit length on D' due to its interaction with D , $f_1' = 0$, $f_3' = 0$, and

$$f_2' = 2b^2 [C_2^* + C_1^* + (C_2^* - C_1^*) \cos 2\alpha] w^{-1}. \quad (4.1.12)$$

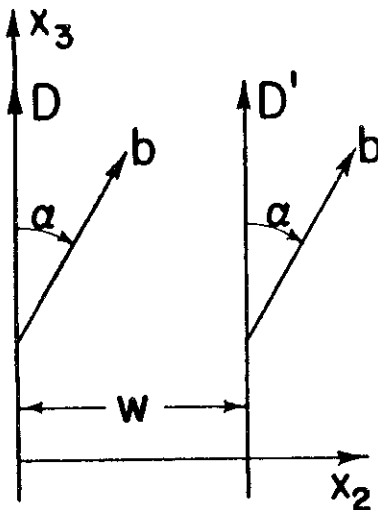


Figure 5. Schematic drawing of dislocations with equal Burgers vectors.

4.2. Stacking Fault Energy and Width of Extended Dislocations

According to current theory the equilibrium separation of the two partials of an extended dislocation depends in part on their elastic interaction, and there must necessarily be a certain amount of distortion from perfect stacking fault positions in the entire region between the partials. For this reason, the average stacking fault energy per unit area must be a function

$\gamma_F(w, \alpha)$ of the width w of the extended dislocation and of the angle α between the dislocation and the total Burgers vector. As w becomes much greater than the diameter of the core of a partial dislocation, this function asymptotically approaches a constant value γ_F . Equating the decrease in elastic energy in a small virtual increase in w to the increase in stacking fault energy gives the well-known conditions of equilibrium:

$$\gamma_F = f(w, \alpha) \quad , \quad (4.2.1)$$

where f is the force of repulsion per unit length of the partial dislocations due to their elastic interaction.

4.2.1. Analytical Results

For extended dislocations in the basal plane of hexagonal crystals (4.2.1) and (4.1.5) yield

$$\gamma_F w = b_p^2 [C_2^* + C_1^* + 2(C_2^* - C_1^*) \cos 2\alpha] \quad , \quad (4.2.2)$$

in which the c_{ij} to be used are given by (I.2.2). It is sometimes convenient to write this as

$$\gamma_F w_{45^\circ} = b_p^2 (C_1^* + C_2^*) \quad (4.2.3)$$

and

$$w = \left(1 - 2 \frac{C_1^* - C_2^*}{C_1^* + C_2^*} \cos 2\alpha \right) w_{45^\circ} \quad , \quad (4.2.4)$$

where w_{45° is the width of a 45° extended dislocation and also is the average width of extended dislocations.

For extended dislocations in any of the (111) family of planes in face-centered cubic crystals (4.2.1) and (4.1.10) yield

$$\gamma_F w = b_p^2 \left[C_2^* + C_1^* \frac{1 + 2\delta_1}{3} + 2 \left(C_2^* - C_1^* \frac{1 + 2\delta_1}{3} \right) \cos 2\alpha \right] \quad , \quad (4.2.5)$$

in which the c_{ij} to be used are given by (I.2.4). From the derivation of (4.1.10) it follows that this formula is exact only for $\alpha = 0^\circ$ and 60° , screw and 60° extended dislocations. However, because of the pseudo-isotropic properties of a (111) plane, (4.2.5) should be a good approximation for all α with a maximum error of about 10 per cent. This estimate of error is based on the

known error of a similar approximation formula, (3.1.2), for the line energy of a dislocation in a (111) plane, as discussed in Section 3.2.2.

4.2.2. Numerical Results

The numerical values of the product $\gamma_F w$ of stacking fault energy times width of an extended dislocation are given in Table 3 for several substances

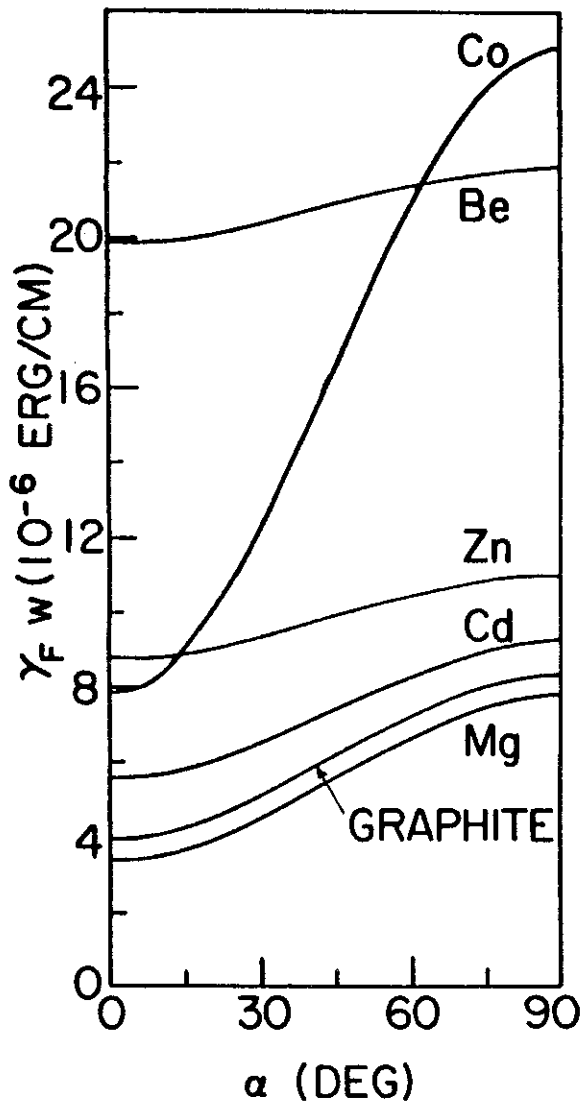
TABLE 3
STACKING FAULT ENERGY TIMES DISLOCATION WIDTH

| Substance | $\gamma_F w (10^{-6} \text{ erg/cm})$ | | | | | $\frac{w_{90^\circ}}{w_0^\circ}$ |
|---------------------------------------|---------------------------------------|---------------------|---------------------|---------------------|---------------------|----------------------------------|
| | $\alpha = 0^\circ$ | $\alpha = 30^\circ$ | $\alpha = 45^\circ$ | $\alpha = 60^\circ$ | $\alpha = 90^\circ$ | |
| <u>Hexagonal Crystals¹</u> | | | | | | |
| Graphite | 4.0 | 5.1 | 6.2 | 7.3 | 8.4 | 2.1 |
| Be | 19.9 | 20.4 | 20.9 | 21.4 | 21.9 | 1.10 |
| Cd | 5.60 | 6.51 | 7.42 | 8.33 | 9.24 | 1.65 |
| Co | 7.92 | 12.20 | 16.49 | 20.78 | 25.07 | 3.17 |
| Mg | 3.41 | 4.51 | 5.61 | 6.71 | 7.81 | 2.29 |
| Zn | 8.80 | 9.35 | 9.90 | 10.46 | 11.01 | 1.25 |

| Substance | $\gamma_F w (10^{-6} \text{ erg/cm})$ | | | | | $\frac{w_{90^\circ}}{w_0^\circ}$ |
|---|---------------------------------------|---------------------|---------------------|---------------------|---------------------|----------------------------------|
| | $\alpha = 0^\circ$ | $\alpha = 30^\circ$ | $\alpha = 45^\circ$ | $\alpha = 60^\circ$ | $\alpha = 90^\circ$ | |
| | Exact | Approx. | Approx. | Exact | Approx. | Approx. |
| <u>Face-Centered Cubic Crystals¹</u> | | | | | | |
| Ag | 3.38 | 5.88 | 8.37 | 10.87 | 13.36 | 3.95 |
| Al | 4.00 | 5.57 | 7.14 | 8.71 | 10.28 | 2.57 |
| Au | 2.65 | 5.48 | 8.32 | 11.16 | 14.00 | 5.29 |
| Cu | 4.38 | 7.25 | 10.12 | 13.00 | 15.87 | 3.63 |
| Ni | 8.84 | 12.73 | 16.61 | 20.50 | 24.38 | 2.76 |
| Pb | 1.08 | 2.37 | 3.66 | 4.95 | 6.24 | 5.77 |

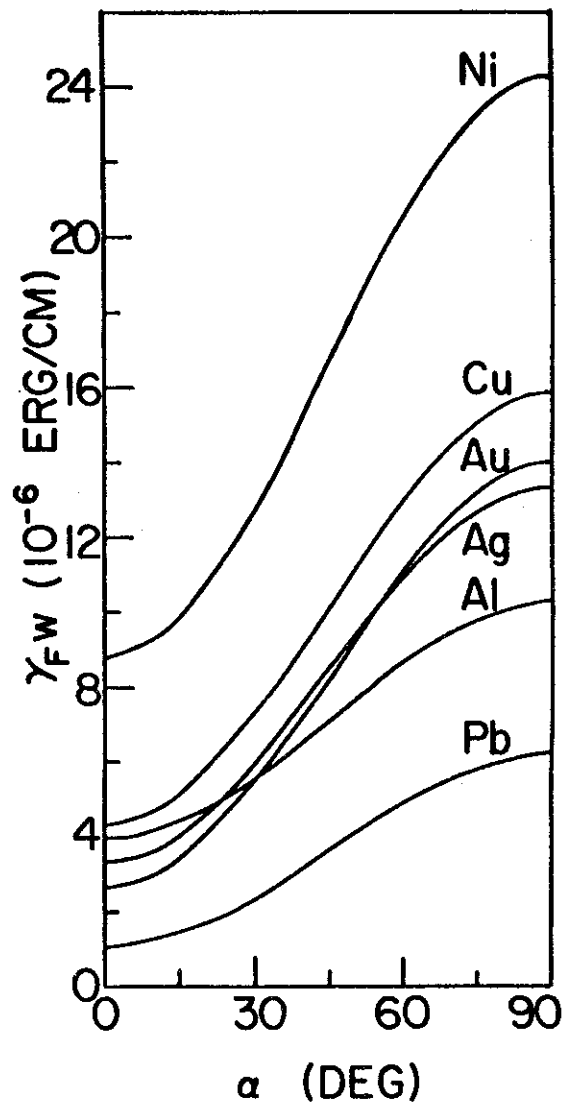
¹ Based on elastic constants given in Table 5.

of hexagonal and face-centered cubic symmetry for the elastic constants given in Table 5 (Appendix I). The accuracy is the same as that of Table 2, discussed in Section 3.2. The angle α is the angle between the dislocation line and the total Burgers vector of the extended dislocation. The variation of the product $\gamma_F w$ with α is shown in Figures 6 and 7. Since γ_F is a constant,



N-2256

Figure 6. Stacking fault energy times width of extended dislocation versus orientation.



N-2257

Figure 7. Approximate value of stacking fault energy times width of extended dislocation versus orientation.

these graphs essentially show the variation in width of an extended dislocation with orientation relative to its Burgers vector. As discussed in the preceding section, the curves for face-centered cubic crystals are exact only at α equal 0° and 60° .

The product $\gamma_F w$ for graphite has about the same range as for other metals. Therefore, the large width of extended dislocations in graphite is due to its low stacking fault energy and not to unusually strong forces of repulsion between dislocations. As noted in Table 3, the width of an edge dislocation in graphite is about 2.1 times the width of a screw dislocation.

Read (11) reports that for isotropic crystals the ratio w for edge to w for screw dislocations is $(2 + \nu)/(2 - 3\nu)$, which is about 2 for typical values of Poisson's ratio. As shown in Table 3 this ratio varies from 1.1 for Be to 5.8 for Pb, for the twelve materials studied. The ratio is greater than 2 for all the face-centered cubic metals studied. The deviation of these values from the results of isotropic theory depends on what criteria are used to choose values for the shear modulus G and Poisson's ratio. For graphite the isotropic theory with $G = c_{44}$ and $\nu = 1/3$ gives results which are low by a factor of about 13. For metals the isotropic theory is in error from 0 to 80 per cent with 30 per cent being typical.

The derivation of $\gamma_F w$ is based on the assumption that the cores of the partials do not interact. From Figures 6 and 7 it is seen that this should not be valid for materials with stacking fault energies greater than about 100 ergs/cm², such as Al, Cd, and Zn (γ_F for Be and Mg is unknown and for Ni is variously reported as from 100 to 400 ergs/cm²). An estimate of the effect of neglecting the core interactions can be made by comparing the present results with those of Seeger and Schöck (4, 12). Their method treats the core interactions approximately by making a simple assumption as to the Peierls force between atoms on opposite sides of the slip plane. The elastic field elsewhere is treated rigorously by the anisotropic elastic continuum theory. Table 4 gives

TABLE 4
COMPARISON WITH RESULTS OF SEEGER AND SCHÖCK for $\gamma_F w$

| Substance | $\gamma_F w$ for Screw Dislocation ¹ | | | $\gamma_F w$ for Edge Dislocation ¹ | | |
|-----------|---|-------------------|---------------------|--|-------------------|---------------------|
| | Seeger Schöck | Present Theory | Isotropic Theory | Seeger Schöck | Present Theory | Isotropic Theory |
| Al | 6.3 | 4.0 | 4.0 | 8.6 | 10.3 | 9.4 |
| Cu | 4.6 | 4.5 | 6.1 | 12.2 | 15.7 | 12.3 |
| Ni | 7.4 | 8.1 | 8.6 | 23.9 | 23.7 | 20.0 |
| Co | 8.8 | 5.9 | 6.4 | 39.6 | 18.0 | 15.0 |

¹ $\gamma_F w$ in units of 10^{-6} erg/cm.

the value of $\gamma_F w$ obtained by Seeger and Schöck and the values given by the present theory and by isotropic theory for the same elastic constants as used by Seeger and Schöck. For the isotropic theory Poisson's ratio was taken as $\nu = 1/3$. For face-centered cubic crystals the shear modulus $G = (c_{11} - c_{12} + c_{44})/3$ for shear across a (111)-type plane was used; and for hexagonal crystals $G = c_{44}$ for shear across the basal plane was used.

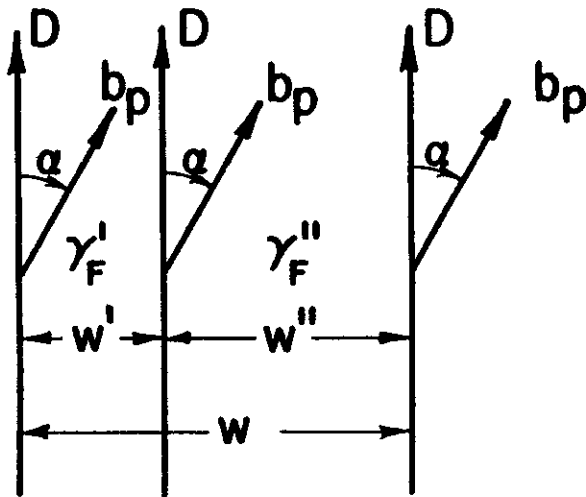
The stacking fault energy of Co is about 25 ergs/cm². This gives $w > 24A$ for a screw dislocation and $w > 72A$ for an edge dislocation. If, as seems reasonable, there is negligible core interaction at these distances, then Seeger and Schöck's theory and the present theory should give identical results. The rather large discrepancy for the edge dislocation raises some question as to the validity of the approximations used by Seeger and Schöck. For Al the partials are separated by less than 5A and there should be considerable core interaction. Assuming Seeger and Schöck's values are correct, we see that the neglect of core interactions in the present theory causes an error of 20 to 30 per cent. This should be taken into consideration when applying the present theory to other materials of high stacking fault energy. It is of interest to note by a comparison of Tables 3 and 4 that the change in $\gamma_F w$ for Ni and Co due to changes in the elastic constants used is of the same order as the difference between the isotropic and anisotropic results.

In summary it is suggested that the present theory is essentially as easy to apply as the isotropic theory and will give more accurate results except possibly in the case of strongly interacting cores. The use of more accurate theories is only justified if the elastic constants are known accurately and perhaps only if a more accurate treatment of the Peierls force is made than any up to the present.

4.3. Stacking Fault Energy and Width of Triple Partial Ribbons

Amelinckx and Delavignette^(13, 14) have observed extended dislocation ribbons in graphite consisting of three parallel partial dislocations with the same Burgers vector as indicated in Figure 8. They have shown that the triple partial ribbon is formed from the interaction of two extended dislocations lying above nearest neighboring or next nearest neighboring planes. In the first case the ribbon is symmetrical and the stacking fault energies are equal; in the second case the ribbon is unsymmetrical and the stacking fault energies are unequal.

The analysis of Amelinckx and Delavignette for isotropic materials can be easily generalized for anisotropic materials. Since the interlayer distance is only a few angstroms while the widths w' and w'' between partials are several thousand angstroms, we can make the simplifying approximation that all dislocations lie in the same plane. The error caused by this is negligible compared to the present experimental error in determining w' and w'' . Equating the force of repulsion between dislocations with equal Burgers vectors, equation (4.1.12) to the surface tension of the stacking fault yields two independent equations of equilibrium. From these it follows that



N-1570

Figure 8. Schematic drawing of a triple partial ribbon.

$$\gamma_{F'} = B(2 + R^{-1})/w \quad \gamma_{F''} = B(2 + R)/w, \quad (4.3.1)$$

where

$$R = w'/w'' \quad w = w' + w'' \quad (4.3.2)$$

and

$$B = 2b_p^2 [C_2^* + C_1^* + (C_2^* - C_1^*) \cos 2\alpha] . \quad (4.3.3)$$

Also,

$$\frac{\gamma_{F''}}{\gamma_{F'}} = \frac{2 + R}{2 + R^{-1}} . \quad (4.3.4)$$

Equations (4.3.1) and (4.3.2) yield

$$w' = 3B / (2\gamma_{F'} - \gamma_{F''} + \sqrt{\gamma_{F'}^2 - \gamma_{F'}\gamma_{F''} + \gamma_{F''}^2}) \quad (4.3.5)$$

$$w'' = 3B / (2\gamma_{F''} - \gamma_{F'} + \sqrt{\gamma_{F'}^2 - \gamma_{F'}\gamma_{F''} + \gamma_{F''}^2}) \quad (4.3.6)$$

$$w = B(\gamma_{F'} + \gamma_{F''} + \sqrt{\gamma_{F'}^2 - \gamma_{F'}\gamma_{F''} + \gamma_{F''}^2}) / \gamma_{F'}\gamma_{F''} . \quad (4.3.7)$$

These formulas differ from those for the isotropic case only in the definition of B. For triple partial ribbons in the basal plane of hexagonal crystals the c_{ij} to be used are given in terms of the standard elastic constants by (1.2.2).

For a symmetrical triple partial ribbon $\gamma_{F'} = \gamma_{F''} = \gamma_F$ and

$$w = 3B/\gamma_F . \quad (4.3.8)$$

Comparison with (4.2.3) shows that the average width $w_{45^\circ, \text{rib}}$ at $\alpha = 45^\circ$ of a symmetrical triple partial ribbon is related to the average width $w_{45^\circ, \text{ext}}$ of an extended dislocation of equal stacking fault energy by

$$w_{45^\circ, \text{rib}} = 6w_{45^\circ, \text{ext}} \quad (4.3.9)$$

The factor of 6 does not exist at other orientations, but

$$w_{0^\circ, \text{rib}} = 6w_{30^\circ, \text{ext}} \quad \text{and} \quad w_{90^\circ, \text{rib}} = 6w_{60^\circ, \text{ext}} \quad (4.3.10)$$

Thus, the width of screw and edge symmetrical triple partial ribbons can be obtained easily from Table 3.

4.4. Stacking Fault Energy and Radius of Extended Nodes

Whelan ⁽¹⁵⁾ has shown that the stacking fault energy can be estimated by equating the surface tension of the stacking fault to a force due to the line tension U of a partial dislocation and the radius of curvature r of an extended node, according to the formula

$$\gamma_F = U/r \quad (4.4.1)$$

The line tension may be estimated by assuming that it is the same as the line energy per unit length of the elastic stress field of a dislocation. As discussed in Section 3.1, the line energy within a cylinder of outer radius R and inner radius r_0 can be calculated from (3.1.1) and subsequent formulas in which b is the magnitude b_p of the Burgers vector of a partial dislocation and α is the angle between the Burgers vector and the partial dislocation at its midpoint. Reference should be made by Section 3 for further details and numerical values.

The major difficulty in applying (4.4.1) and (3.1.1) is in estimating the factor $\ln R/r_0$. Presumably, R is approximately the average distance between total dislocations and r_0 is approximately b_p ; but there is no unique way of determining these quantities.

4.5. Stacking Fault Energy of Graphite

In the three preceding sections, formulas based on anisotropic elasticity theory have been presented for estimating the stacking fault energy of graphite from the width of an extended dislocation, from the width of a triple partial ribbon, and from the radius of curvature of a large extended node. All three of these lengths can be obtained from electron micrographs of dislocations in thin films of graphite. In this section we shall neglect the effect of the stress-free surfaces of the thin films on the widths and radius of curvature; and assume that the observed lengths are the same as those in an infinite crystal.

Williamson ⁽¹⁶⁾ and Amelinckx and Delavignette ⁽¹³⁾ have reported that the average width of extended dislocations is about 1000 Å. From Table 3, $\gamma_F w_{45^\circ} = 6.2 \times 10^{-6}$ erg/cm so $\gamma_F = 0.62$ erg/cm². From observations on single, gently curving extended dislocations Siems, Delavignette, and Amelinckx ⁽¹⁷⁾ report that within their experimental error w varies as $\cos 2\alpha$ with $w_{90^\circ}/w_{0^\circ} = 2.6$ and $w_{45^\circ} = 850$ Å, for which the present theory gives $\gamma_F = 0.73$ erg/cm². The present theory predicts that $w_{90^\circ}/w_{0^\circ} = 2.1$.

Delavignette and Amelinckx⁽¹⁸⁾ have observed symmetrical triple partial ribbons with average total widths of $w_0^\circ = 5300\text{A}$ and $w_{60^\circ} = 7000\text{A}$, which by (4.3.8) both yield a value of γ_F of 0.58 erg/cm^2 . The exact agreement is fortuitous, as the uncertainty in γ_F is roughly ± 20 per cent.

In Sections 5.2 and 5.3 we shall show that the effect of the stress-free surfaces of the thin films is to reduce the width of dislocations. At present the experimental data are too incomplete to draw definite conclusions. It appears that the change in widths of extended dislocations and triple partial ribbons in the thin films used in electron microscopy may be up to roughly 10 per cent smaller than the width in an infinite crystal. The calculated stacking fault energy might be 10 per cent less than the values given above, due to this effect.

On electron micrographs taken by Williamson and by Amelinckx and Delavignette, the radius of curvature of extended nodes has varied from 0.9 to 1.7 μ . Where it has been measured, the partials have been in screw orientation at their midpoint; the average distance between dislocations is roughly 1 μ . Taking $\alpha = 0^\circ$, $R = 1 \mu$, and $r_0 = b_p = 1.42\text{A}$, we find from (4.4.1) and (3.1.2) that γ_F is from 0.25 to 0.50 erg/cm^2 . These computed values of γ_F should be less than the true value because the repulsion between the three partials in an extended node has been neglected in the theory. It appears that all three methods of determining the stacking fault energy in graphite give results which are consistent with the value

$$\gamma_F = 0.6 \pm 0.2 \text{ erg/cm}^2 \quad (4.5.1)$$

Numerous measurements of widths of extended dislocations and triple partial ribbons have been made on electron micrographs taken at this laboratory by R. Bacon and R. Sprague. As the orientation of the dislocations was not determined, only the general range of dislocation widths can be determined. Several extended dislocations indicate an average width in the 800 to 900A range, and a few symmetrical triple partial ribbons indicate an average width in the 0.5 to 0.6 μ range, in agreement with the results of others. However, the experimental results are not as simple as indicated above. Several well-isolated dislocations with widths in the 1500 to 2000A range were observed. On some plates with a dislocation spacing of a few thousand Angstrom, the widths of extended dislocations varied from 1000 to 3000A and some symmetrical triple partial ribbons occurred with widths from 2000 to 4000A. These anomalous widths occurred for a considerable range of orientations on a given micrograph. Further work is being done to attempt to determine which of several possible causes is responsible for these results.

5. INFLUENCE OF A STRESS-FREE SURFACE ON DISLOCATION WIDTHS

Three cases for which the influence of stress-free, plane surfaces on the widths of dislocations can be easily determined are considered in this chapter. The first is that of an extended dislocation in any orientation lying parallel to the plane surface of a semi-infinite isotropic solid. The second and third are those of a 30° extended dislocation and of a screw triple partial ribbon lying parallel to the plane surfaces of an anisotropic crystalline plate for which the elastic constants are of Type I.

5.1. Arbitrary Extended Dislocation in a Semi-Infinite Isotropic Solid

Dietze and Leibfried ⁽¹⁹⁾ have calculated the stress components of an edge dislocation lying parallel to the parallel, plane surfaces of an isotropic plate of infinite lateral dimensions. Simple formulas in closed form suitable for analytical applications could not be found. However, they did obtain simple formulas for the stress components of an edge dislocation lying parallel to the single plane surface of a semi-infinite isotropic solid. The effect of the stress-free surface on the dislocation width in a semi-infinite solid should illustrate qualitatively the effect that the stress-free surfaces of thin films or plates have on the dislocation widths observed in electron microscopy.

Let a be the distance of the extended dislocation from the stress-free surface, as indicated in Figure 9. The Burgers vectors are as shown in

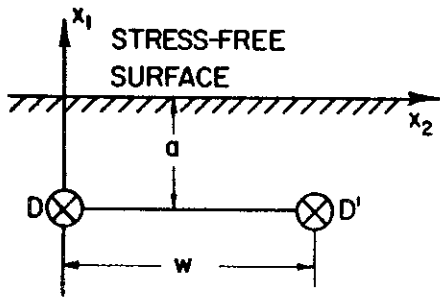


Figure 9. Coordinate system for an extended dislocation in a semi-infinite solid.

Figure 3. The plane $x_1 = 0$ is the stress-free surface of the semi-infinite isotropic solid. Eshelby ⁽²⁰⁾ has shown that the force per unit length on D' due to its interaction with D and the stress-free surface is given by (4.1.2) in which the $\tau_{ij} = \tau_{ij}^\infty + \tau_{ij}^I$ are the components of the total stress field due to the partial dislocation D acting alone. The τ_{ij}^∞ are the components of the stress field of D in an infinite body. The τ_{ij}^I , called the image stress-field components, represent a stress field with no singularities within the body and which is equal in magnitude but opposite in sign to τ_{ij}^∞ on the stress-free boundaries. For screw dislocations the singularities of τ_{ij}^I can be interpreted as image dislocations; but for edge dislocations this interpretation and the corresponding method of calculation are not possible.

Dietze and Leibfried ⁽¹⁹⁾ give

$$\tau_{11} = C_1 b_2 \left[\frac{(x_1 + a) [(x_1 + a)^2 - x_2^2]}{[(x_1 + a)^2 + x_2^2]^2} - \frac{(x_1 - a) [(x_1 - a)^2 - x_2^2]}{[(x_1 - a)^2 + x_2^2]^2} - 2a \frac{(3x_1 - a)(x_1 - a)^3 - 6x_1(x_1 - a)x_2^2 - x_2^4}{[(x_1 - a)^2 + x_2^2]^3} \right] \quad (5.1.1)$$

$$\tau_{12} = C_1 b_2 \left[\frac{x_2 [(x_1 + a)^2 - x_2^2]}{[(x_1 + a)^2 + x_2^2]^2} - \frac{x_2 [(x_1 - a)^2 - x_2^2]}{[(x_1 - a)^2 + x_2^2]^2} - 4a x_1 x_2 \frac{3(x_1 - a)^2 - x_2^2}{[(x_1 - a)^2 + x_2^2]^3} \right] \quad (5.1.2)$$

$$\tau_{22} = C_1 b_2 \left[\frac{(x_1 + a) [(x_1 + a)^2 + 3x_2^2]}{[(x_1 + a)^2 + x_2^2]^2} - \frac{(x_1 - a) [(x_1 - a)^2 + 3x_2^2]}{[(x_1 - a)^2 + x_2^2]^2} + 2a \frac{(x_1 + a)(x_1 - a)^3 - 6x_1(x_1 - a)x_2^2 + x_2^4}{[(x_1 - a)^2 + x_2^2]^3} \right] \quad (5.1.3)$$

$$\tau_{13} = C_2 b_3 \left[-\frac{x_2}{(x_1 + a)^2 + x_2^2} + \frac{x_2}{(x_1 - a)^2 + x_2^2} \right] \quad (5.1.4)$$

$$\tau_{23} = C_2 b_3 \left[\frac{x_1 + a}{(x_1 + a)^2 + x_2^2} - \frac{x_1 - a}{(x_1 - a)^2 + x_2^2} \right] \quad (5.1.5)$$

$$\tau_{33} = \nu(\tau_{11} + \tau_{22}), \quad (5.1.6)$$

in which C_1 and C_2 are given by (2.2.12) and (2.2.13). The formulas for an edge dislocation have also been derived by Head⁽²¹⁾.

Equating the stacking fault energy per unit area γ_F to f_2^1 and evaluating f_2^1 by (4.1.2), (5.1.2), and (5.1.4), we get

$$\gamma_F = \frac{a^2 G b_p^2}{2\pi(1-\nu)w(w^2 + 4a^2)} \left[2 - \nu - 2\nu \cos 2\alpha + \frac{w^2(3w^2 - 4a^2)}{(w^2 + 4a^2)^2} (1 - 2 \cos 2\alpha) \right]. \quad (5.1.7)$$

In the limit $a \rightarrow \infty$ this reduces to the known formula

$$\gamma_F w_\infty = G b_p^2 (2 - \nu - 2\nu \cos 2\alpha) / 8\pi(1 - \nu), \quad (5.1.8)$$

relating the stacking fault energy to the width w_∞ of an extended dislocation in an infinite, isotropic medium. For our purposes it is convenient to use (5.1.8) to eliminate γ_F from (5.1.7); there results

$$\frac{w}{w_\infty} = \frac{4a^2}{w^2 + 4a^2} \left[1 + \frac{w^2(3w^2 - 4a^2)}{(w^2 + 4a^2)^2} \frac{(1 - 2 \cos 2\alpha)}{(2 - \nu - 2\nu \cos 2\alpha)} \right]. \quad (5.1.9)$$

Since this cannot be solved algebraically to yield the explicit dependence of w on a , we proceed as follows. Measure distances relative to the width of the dislocation in an infinite medium by introducing the dimensionless quantities

$$W = w/w_{\infty} \text{ and } A = a/w_{\infty} \quad . \quad (5.1.10)$$

Define a dimensionless parameter

$$\underline{\Psi} = w/2a = W/2A \quad (5.1.11)$$

and the function

$$g(\underline{\Psi}; \nu, \alpha) = \frac{1}{1+\underline{\Psi}^2} \left[1 + \frac{\underline{\Psi}^2 (3\underline{\Psi}^2 - 1)}{(1+\underline{\Psi}^2)^2} \frac{(1 - 2 \cos 2\alpha)}{(2 - \nu - 2\nu \cos 2\alpha)} \right]. \quad (5.1.12)$$

The dependence of relative width on relative depth from the surface is given parametrically by

$$W = g(\underline{\Psi}; \nu, \alpha) \quad (5.1.13)$$

and

$$A = g(\underline{\Psi}; \nu, \alpha) / 2 \underline{\Psi} \quad . \quad (5.1.14)$$

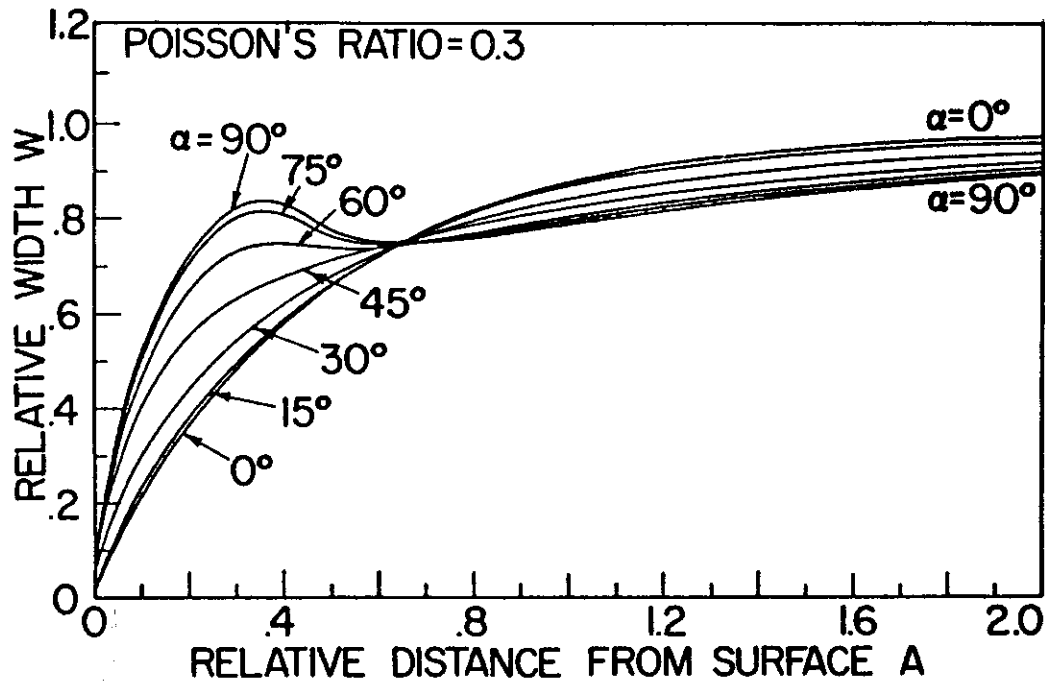
Figure 10 shows the variation in relative width versus relative distance from the surface for Poisson's ratio $\nu = 0.3$ and for several orientations. It follows from (5.1.12) that the curves for 30° and 60° dislocations are independent of ν . The dependence of W on ν for screw and edge dislocations is shown in Figure 11. From these we see that for all orientations of dislocations in all nearly isotropic materials there will be no strong variation in width unless the dislocation is closer than w_{∞} to the surface. As ν decreases from about $0.6 w_{\infty}$ ($3\sqrt{3}/8$ in the isotropic case) toward zero, the relative width of a screw dislocation approaches zero more rapidly than that of an edge dislocation.

Although there are no anomalous variations in width for ν in the range of practical interest, $0 < \nu < 0.5$, there are extreme variations in the width of predominantly screw ($\alpha < 30^\circ$) dislocations if ν is about $2/3$. This is indicated by Figure 12 for a screw dislocation. In this range the width may be much greater than w_{∞} and there may be two positions of stable equilibrium separated by a position of unstable equilibrium (the dashed curve). There has been speculation in the past that the anomalous behavior for large values of ν in isotropic materials might also occur in strongly anisotropic materials. However, there does not seem to be any proven example of this.

5.2. A 30° Extended Dislocation in an Anisotropic Plate

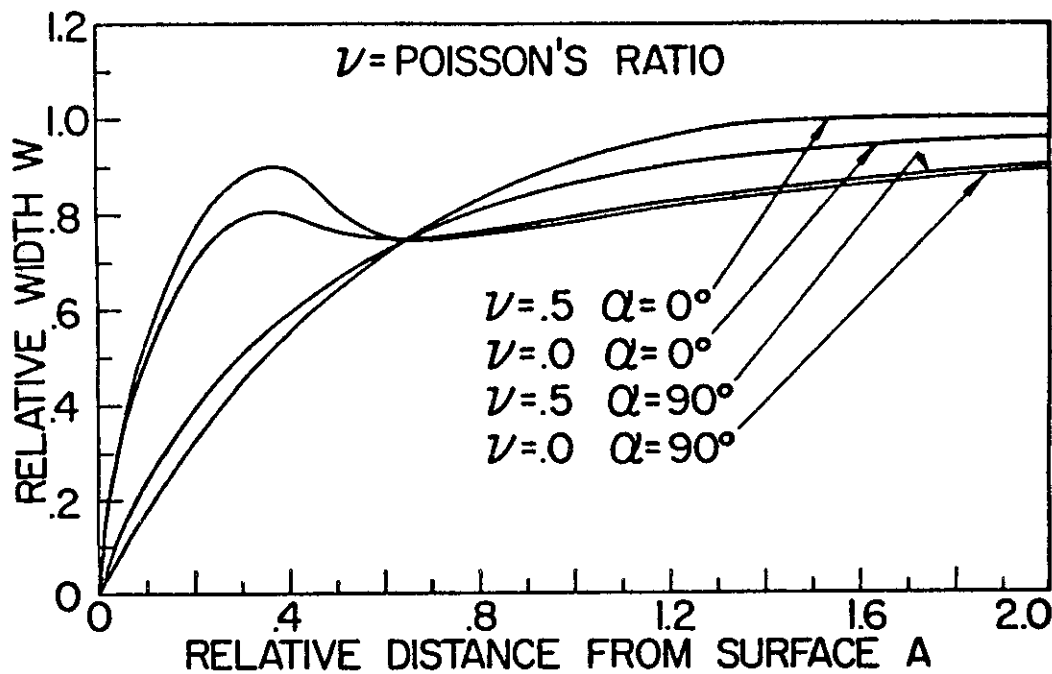
5.2.1. Analytical Results

For a 30° extended dislocation the Burgers vector of one of the two partial



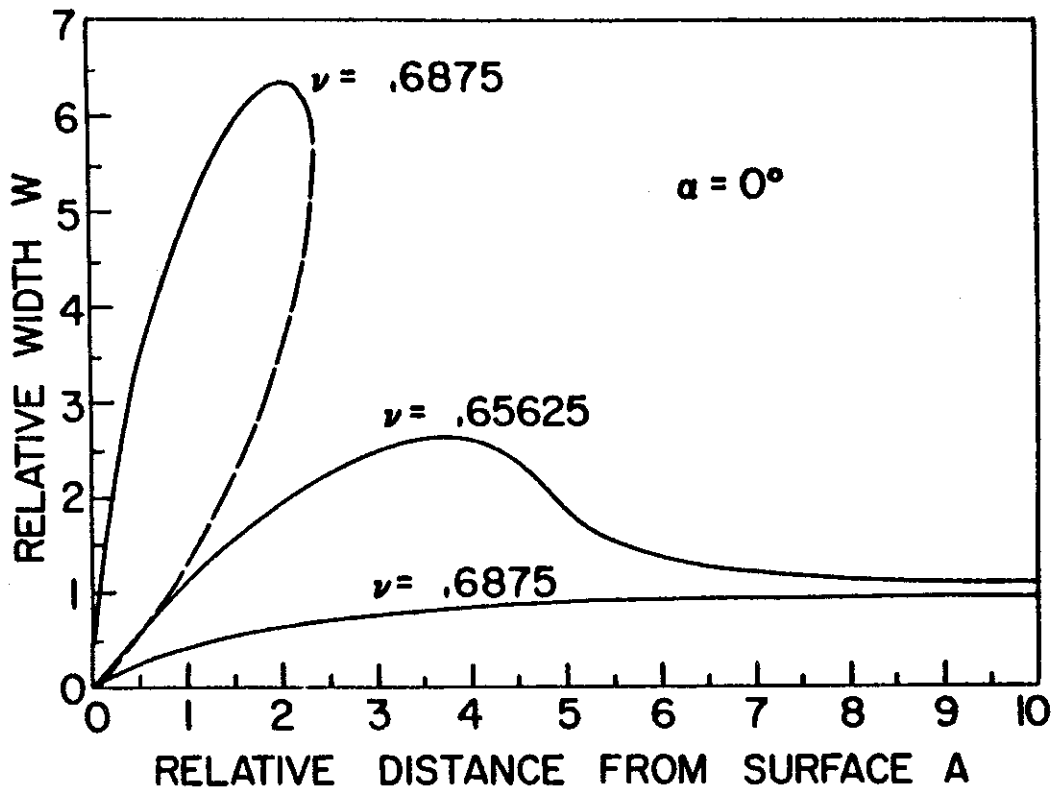
N-1573

Figure 10. Variation in width of a dislocation in a semi-infinite isotropic solid with depth from surface.



N-1574

Figure 11. Variation in width of a dislocation in a semi-infinite isotropic solid with depth from surface.



N-1228

Figure 12. Variation in width of a screw dislocation in a semi-infinite isotropic solid of large ν with depth from surface.

dislocations is in the pure screw orientation, and for Type I elastic constants the partials interact only through the screw components. The stress components for a screw dislocation lying parallel to the surfaces of an anisotropic flat plate were derived in Section 2.3. The coordinate system is shown in Figure 1; except that a second partial dislocation must be added passing through the point $(-a, w, 0)$. Setting $\gamma_F = f_2^1$, we obtain from (4.1.2) and (2.3.6)

$$\gamma_F = \frac{\pi\sqrt{\delta_3} C_2 b_p^2}{4d} \left[\frac{\sinh \pi\sqrt{\delta_3} d^{-1} w}{\cosh \pi\sqrt{\delta_3} d^{-1} w - 1} - \frac{\sinh \pi\sqrt{\delta_3} d^{-1} w}{\cosh \pi\sqrt{\delta_3} d^{-1} w - \cos 2\pi m} \right], \quad (5.2.1)$$

where

$$m = a/d \quad . \quad (5.2.2)$$

Contrails

For hexagonal crystals the c_{ij} to be used are given in terms of the standard elastic constants by formula (I.2.2). In the limit $m = \text{constant}$ and $d \rightarrow \infty$, this reduces to

$$\gamma_F w_\infty = \frac{1}{2} C_2 b_p^2, \quad (5.2.3)$$

relating the width w_∞ of a 30° extended dislocation in an infinite anisotropic crystal to the stacking fault energy. Using (5.2.3) to eliminate γ_F from (5.2.1), we obtain

$$\frac{d}{w_\infty} = \frac{\pi\sqrt{\delta_3}}{2} \left[\frac{\sinh \pi\sqrt{\delta_3} d^{-1} w}{\cosh \pi\sqrt{\delta_3} d^{-1} w - 1} - \frac{\sinh \pi\sqrt{\delta_3} d^{-1} w}{\cosh \pi\sqrt{\delta_3} d^{-1} w - \cos 2\pi m} \right]. \quad (5.2.4)$$

In order to analyze this introduce the relative distances

$$W = w/w_\infty, \quad D = d/w_\infty, \quad \text{and} \quad A = a/w_\infty. \quad (5.2.5)$$

Then

$$m = a/d = A/D. \quad (5.2.6)$$

Solving (5.2.4) for A, we get

$$A = \frac{D}{2\pi} \cos^{-1} \left[\frac{\pi\sqrt{\delta_3} \sinh \pi\sqrt{\delta_3} D^{-1} W - 2D \cosh \pi\sqrt{\delta_3} D^{-1} W (\cosh \pi\sqrt{\delta_3} D^{-1} W - 1)}{\pi\sqrt{\delta_3} \sinh \pi\sqrt{\delta_3} D^{-1} W - 2D (\cosh \pi\sqrt{\delta_3} D^{-1} W - 1)} \right], \quad (5.2.7)$$

which is convenient for computing curves of W versus A at constant D. Alternatively, we can introduce the dimensionless parameter

$$\Omega = \pi\sqrt{\delta_3} w/d = \pi\sqrt{\delta_3} W/D \quad (5.2.8)$$

and define the function

$$f(\Omega, m) = \frac{\sinh \Omega}{2} \left[\frac{1}{\cosh \Omega - 1} - \frac{1}{\cosh \Omega - \cos 2\pi m} \right]. \quad (5.2.9)$$

Then

$$W = \Omega f(\Omega, m) \quad (5.2.10)$$

and

$$D = \pi\sqrt{\delta_3} f(\Omega, m), \quad (5.2.11)$$

which give a parametric form of curves of W versus D at constant m. For a dislocation in the middle of the plate $m = 1/2$ and the formulas reduce to

$$W = \Omega / \sinh \Omega \quad (5.2.12)$$

and

$$D = \pi\sqrt{\delta_3} / \sinh \Omega. \quad (5.2.13)$$

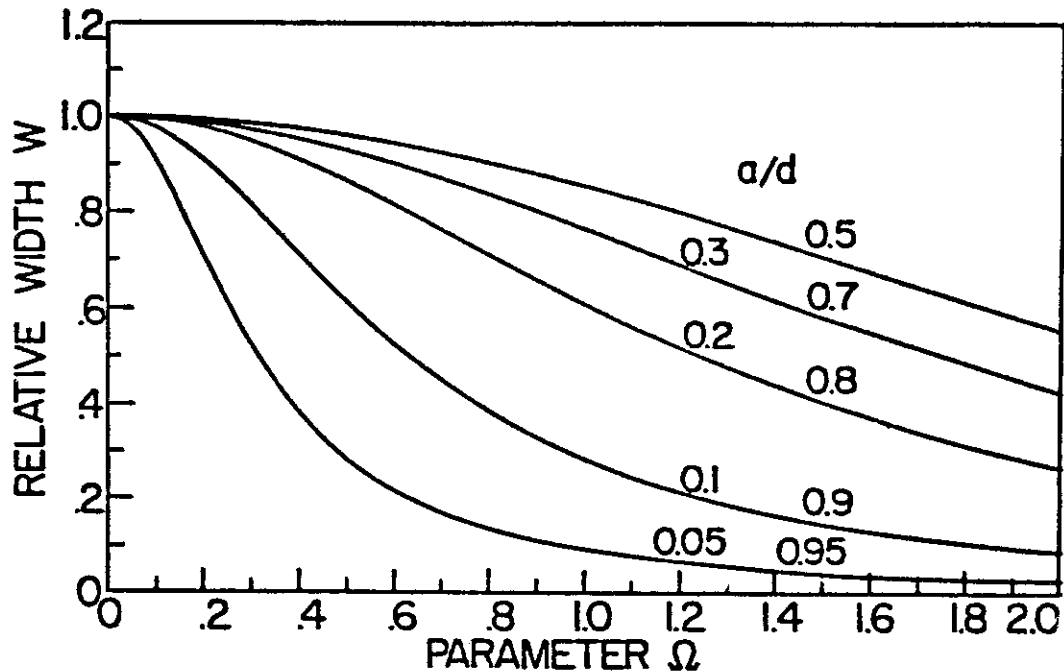
To apply these results to the analysis of 30° extended dislocations observed by electron microscopy it is necessary to measure w , d , and a . Then one can compute, in turn, m , Ω , f , W , and $w_\infty = W/w$; and the stacking fault energy can be determined from (5.2.3). At the present time it seems to be impossible to measure the distance a of the dislocation from the surface. However, for a given plate thickness d the dislocations in the center are widest. Consequently, it should be safe to conclude that $m = 1/2$ for the widest of a large number of experimentally determined dislocation widths in films of the same thickness. Then W can be computed from (5.2.12), and the stacking fault energy obtained as before.

5.2.2. Numerical Results for Graphite

Measurements of w and d for the same film of graphite do not appear to have been made, although this should be possible. Estimates of d for films used by different experimentalists have ranged from, say, 200 to 2000 Å. To get an estimate of the effect of the stress-free surfaces, let us assume that $a = 0.5 d$ for a width of 1000 Å. Using the numerical values of the elastic constants of graphite, we find

$$\Omega = 0.23 w/d \quad . \quad (5.2.14)$$

The W versus Ω curves for several values of a/d are shown in Figure 13 for a

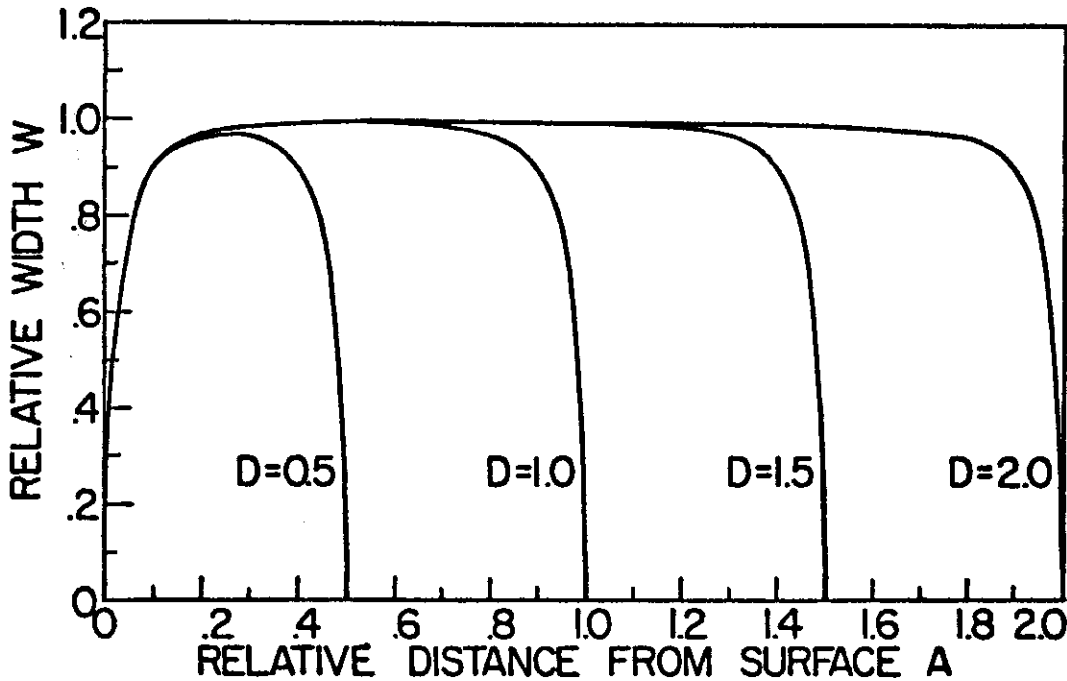


N-1576

Figure 13. Width of a 30° extended dislocation in a graphite plate versus the parameter Ω .

30° extended dislocation in a graphite plate. For $a = 0.5 d$ and, say, $W = 0.90$, the parameter Ω is found to be 0.80; for which $d = 290 \text{ \AA}$. This indicates that the stress-free surfaces decrease the width by less than 10 per cent if d is greater than 300 \AA . If $d > 1000 \text{ \AA}$ and $w = 1000 \text{ \AA}$, then $W > 0.99$. The orientation studies in a semi-infinite solid indicate that this conclusion should be valid for all orientations in a graphite film. On the other hand, if $d < 300 \text{ \AA}$, then there is a significant decrease in the dislocation width which probably depends strongly on the orientation.

Figure 14 shows the variation of W with A for graphite for several film



N-1577

Figure 14. Width of a 30° extended dislocation in a graphite plate as a function of depth from surface and thickness of plate.

thicknesses of interest in electron microscopy. For all $D > 0.5$, the width w is less than $0.9 w_\infty$ only if the dislocation is within $0.1 w_\infty$ of the surface. From the rather flat top of these curves it follows that the widths of almost all dislocations will be within a few per cent of w_∞ in films of thickness $d > 0.5 w_\infty$.

5.3. A Symmetrical, Screw Triple Partial Ribbon in an Anisotropic Plate

5.3.1. Analytical Results

For simplicity we shall consider only the symmetrical, screw triple partial ribbon of total width w . The coordinate system and other notation are the same as in Section 5.2. The single condition of equilibrium is

$$\gamma_F = f_2'(w) + f_2'\left(\frac{w}{2}\right), \quad (5.3.1)$$

where f_2' is given by (4.1.2) and (2.3.6). For Type I elastic constants this yields

$$\gamma_F = \frac{\pi\sqrt{\delta_3} C_2 b_p^2}{2d} \left[\frac{\sinh \pi\sqrt{\delta_3} w/d}{\cosh \pi\sqrt{\delta_3} w/d - 1} - \frac{\sinh \pi\sqrt{\delta_3} w/d}{\cosh \pi\sqrt{\delta_3} w/d - \cos 2\pi m} \right. \\ \left. + \frac{\sinh \pi\sqrt{\delta_3} w/2d}{\cosh \pi\sqrt{\delta_3} w/2d - 1} - \frac{\sinh \pi\sqrt{\delta_3} w/2d}{\cosh \pi\sqrt{\delta_3} w/2d - \cos 2\pi m} \right]. \quad (5.3.2)$$

In the limit $m = \text{constant}$ and $d \rightarrow \infty$, this reduces to

$$\gamma_F w_\infty = 3C_2 b_p^2, \quad (5.3.3)$$

in which w_∞ is the total width of a symmetrical, screw triple partial ribbon in an infinite anisotropic crystal. As in Section 5.2.1 introduce relative distances W , D , and A defined by (5.2.5); Ω defined by (5.2.8); and $f(\Omega, m)$ defined by (5.2.9). Then (5.3.2) and (5.3.3) yield

$$W = 3^{-1} \Omega [f(\Omega, m) + f(\Omega/2, m)] \quad (5.3.4)$$

$$D = 3^{-1} \pi\sqrt{\delta_3} [f(\Omega, m) + f(\Omega/2, m)] \quad (5.3.5)$$

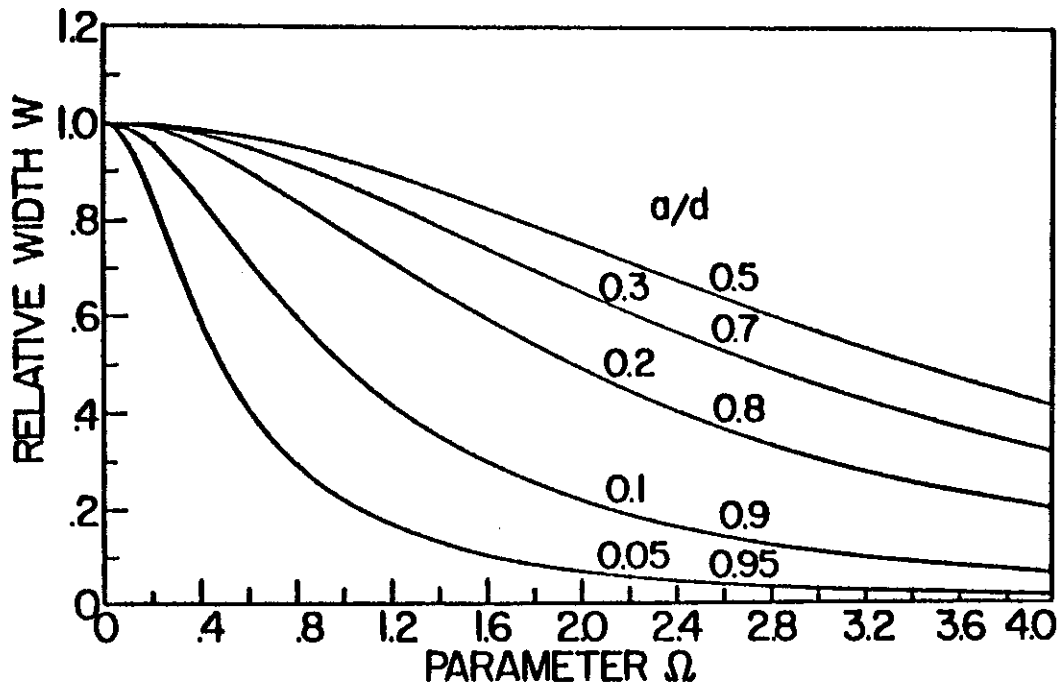
$$A = mD \quad (5.3.6)$$

These results can be applied to the widths of symmetrical, screw triple partial ribbons observed by electron microscopy by the procedure discussed at the end of Section 5.2.1.

5.3.2. Numerical Results for Graphite

The W versus Ω curves for several values of a/d are shown in Figure 15 for a symmetrical, screw triple partial ribbon in a plate of graphite. In order to illustrate the method we shall arbitrarily assume that the 5300 Å wide ribbon observed by Delavignette and Amelinckx⁽¹⁸⁾ was in the center of the film. Then for a 1000 Å thick film, one obtains $\Omega = 1.22$ and from Figure 15 $W = 0.89$. The width in an infinite crystal would be 6000 Å, which by (5.3.3) gives a stacking fault energy of $\gamma_F = 0.51 \text{ erg/cm}^2$. For a 2000 Å thick film, $\Omega = 0.61$ and $W = 0.97$. The width in an infinite crystal would be 5500 Å, which gives a stacking fault energy of $\gamma_F = 0.55 \text{ erg/cm}^2$. These are to be compared with the value of $\gamma_F = 0.58 \text{ erg/cm}^2$ for an uncorrected width of 5300 Å.

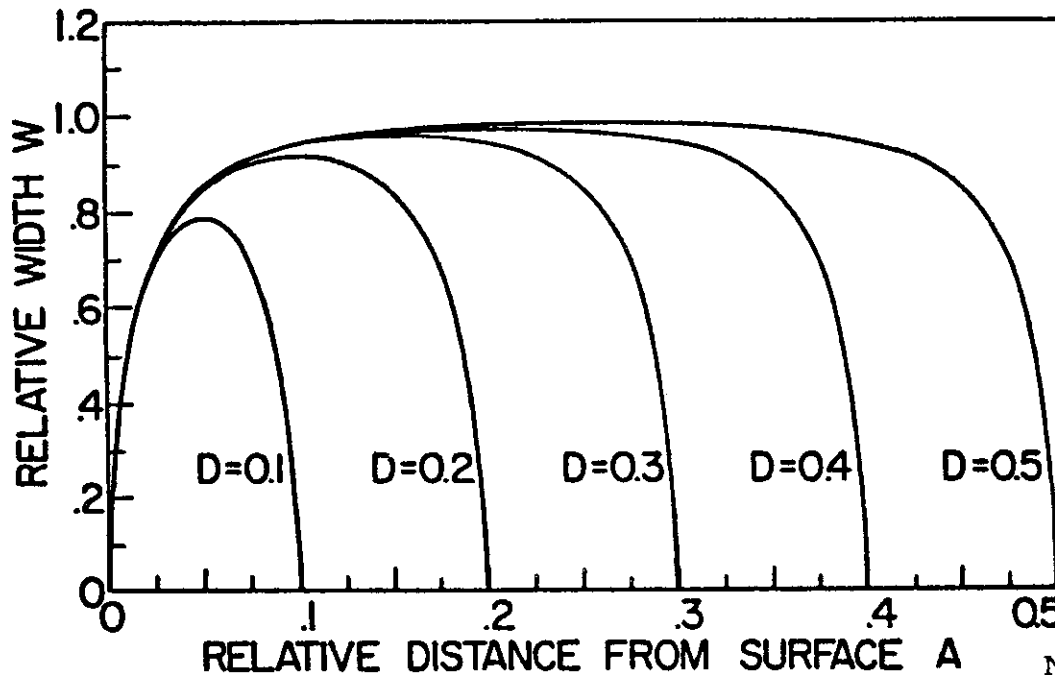
From these results it appears to be desirable to apply a correction to the widths of triple partial ribbon observed in films less than about 2000 Å thick.



N-1578

Figure 15. Width of a symmetrical, screw triple partial ribbon in a graphite plate versus the parameter Ω .

Figure 16 shows the variation of W with A for several film thicknesses



N-1579

Figure 16. Width of a symmetrical, screw triple partial ribbon in a graphite plate as a function of depth from surface and thickness of plate.

of interest in electron microscopy. For a film thickness of 1000 Å, D is about 0.2. The curves of W versus A are not so flat topped as the curves of Figure 14 for extended dislocations. Consequently, it is necessary to observe a larger number of triple partial ribbons to be sure that the widest of these lies at or close to the center of the film.

6. SUMMARY AND CONCLUSIONS

This report presents results of a theoretical study of dislocations based on the linear, anisotropic elastic continuum approximation. The main results fall into three groups: the derivation of formulas not involving complex numbers of stress and displacement components of dislocations in certain symmetry directions, the application of these formulas to derive the relation between stacking fault energy and width of extended dislocations, and a study of the effect which a stress-free surface has on the width of extended dislocations lying parallel to the surface.

Formulas are given for the stress and displacement components of dislocations in the basal plane of a hexagonal crystal, along cube edges or face diagonals in cubic crystals, and in certain other directions. These formulas have the same functional form as in the isotropic case except for the occurrence of dimensionless parameters which are ratios of the elastic stiffness constants and which arise because the different Cartesian coordinates are not equivalent in an anisotropic crystal. Also, formulas are given for the stress and displacement components of a screw dislocation in certain symmetry directions in an anisotropic flat plate with stress-free surfaces.

Formulas already given in the literature for the energy per unit length of the elastic field outside the core of a dislocation are evaluated for graphite and several metals. It is shown that these formulas, although exact only for symmetry directions, are not more than about 10 per cent in error for any direction of the dislocation in a (111) plane in face-centered cubic crystals. Consequently, such formulas should be a considerable improvement over formulas for isotropic materials for estimating stacking fault energy from radii of curvature of extended nodes. The numerical values of the elastic field energy of different types of dislocations in graphite show a much wider variation than in hexagonal metals. The fact that the elastic field energy is not smallest for the most commonly observed type of dislocation in graphite indicates that the core energy and Peierls stress may be as important as the elastic field energy in determining the equilibrium configuration of dislocations in graphite.

From the stress components, formulas are derived for the components of the force of interaction between parallel dislocations with arbitrary Burgers vectors lying in certain symmetry directions. Formulas relating the stacking fault energy to the width and orientation of extended dislocations and triple partial ribbons are derived from the force of repulsion between partial dislocations. These calculations neglect the interactions of the cores of the partial dislocations. That this is probably legitimate except for metals of very

high stacking fault energy is shown by comparing the results given by the present theory with the results of Seeger and Schöck who treated the core interactions of several metals in an approximate way.

The stacking fault energy of graphite has been calculated from the widths of extended dislocations, from the widths of triple partial ribbons, and from the radii of curvature of extended nodes, as reported by experimentalists from observations of electron micrographs of dislocations in graphite. All three methods give results which are compatible with the value 0.6 ± 0.2 erg/cm². The probable error is only an estimate based in part on uncertainties in the values of the elastic constants of graphite and in part on an estimate of the experimental error in determining widths and radii of curvature.

The variation of the width of an extended dislocation with depth from the surface has been calculated for an extended dislocation lying parallel to the stress-free, plane surface of a semi-infinite isotropic solid for all orientations from screw to edge. When the dislocation is at a distance from the surface greater than $0.65 w_{\infty}$, where w_{∞} is the width in an infinite medium, the width is reduced by less than 25 per cent of w_{∞} for all orientations. As the distance from the dislocation to the surface is decreased to zero, the width of a screw dislocation monotonically decreases to zero but the width of an edge dislocation at first decreases, then increases, and finally decreases to zero. These results are valid for all values of the elastic constants of an isotropic material and should be typical of the behavior of an extended dislocation near a stress-free surface of a nearly isotropic metal.

From the stress components, mentioned above, of a screw dislocation lying parallel to the stress-free surfaces of an anisotropic flat plate, the variation of width with depth from surface has been derived for a 30° extended dislocation and for a symmetrical, screw triple partial ribbon. The effect of the surfaces is considerably less for dislocations in graphite with the basal plane parallel to the surface of the plate than for dislocations in isotropic solids. This is due to the fact that the strain field of a dislocation in graphite decreases more slowly along a direction in the slip plane and more rapidly along a direction perpendicular to the slip plane than in a metal. The present theory indicates that the stress-free surfaces will cause the widths of 30° extended dislocations and symmetrical, screw triple partial ribbons in the middle of a graphite plate to be less than 90 per cent of the width in an infinite crystal only in plates thinner than 300 Å for the extended dislocation and 1000 Å for the ribbon. It appears that, except for the thinnest films of graphite used in electron microscopy, the observed widths of extended dislocations of all orientations are within a few per cent of the widths in an infinite crystal. On the other hand, except in the very thickest films of graphite used in electron microscopy, the observed widths of triple partial ribbons are significantly less than the widths in infinite crystals. Definite procedures are given for deriving the widths in an infinite crystal from the observed widths in thin films for 30° extended dislocations and symmetrical, screw triple partial ribbons lying along certain symmetry directions.

The calculation of the stacking fault energy by different methods, the variation in width of dislocations and ribbons with orientation, and the effect of the surfaces of thin films are phenomena which can be accurately checked by

Contrails

experimental observations with the electron microscope. This provides an unusual opportunity to either verify the correctness of the anisotropic elastic continuum theory of dislocations as here applied or else to show that other factors must also be considered. For example, even in annealed crystals the equilibrium positions of partial dislocations may be influenced by the local stresses of point imperfections, the long range thermal and applied stresses, and the fact that the crystals may warp or be small enough in lateral extent that the crystal edges perpendicular to the basal plane must be considered. In view of the widespread use of thin film microscopy to infer the behavior of dislocations in bulk material, it is important to determine all the factors which strongly influence the dislocations.

APPENDIX I
ELASTIC CONSTANTS

I.1 Derivation of Coordinate Systems for Types I or II Elastic Constants

That the sufficient conditions for Types I and II elastic constants given in the literature are not necessary is illustrated by a simple example. In a cubic crystal the elastic constants are Type I if the dislocation is along a face diagonal and the x_1 axis is along a cube edge. Yet in crystal classes 23 and $m\bar{3}$ the face diagonal is neither a twofold axis or perpendicular to a reflecting plane.

Since it does not seem to be possible to find simple necessary and sufficient conditions based on symmetry for the occurrence of Type I or II elastic constants, it is of interest to outline an elementary procedure for finding such systems based on the transformation properties of the elastic stiffness constants. The following analysis applies to all classes of all crystal systems except the cubic system. The cubic system will not be treated in detail since the elastic constants of cubic crystals for different coordinate orientations are given in the literature. Except in the sense already discussed for the cubic system, no other cases of Type I or II elastic constants were found which are not given by the sufficient conditions for these constants cited in the literature.

Let the crystallographic axes be denoted by X_1, X_2, X_3 and let the standard, tabulated elastic stiffness constants, defined with respect to the crystallographic axes, be denoted by c_{ij}^0 . In all crystal systems except cubic c_{33}^0 is greater than zero and unequal to any other standard elastic constant. Therefore, a necessary condition for Type I or II elastic constants is that the six elastic constants $c_{14}, c_{15}, c_{24}, c_{25}, c_{46}$, and c_{56} , defined with respect to a rotated Cartesian coordinate system x_1, x_2, x_3 , must not depend on c_{33}^0 . If the two coordinate systems are related by

$$x_i = \sum_j \beta_{ij} X_j \quad (i, j = 1, 2, 3) \quad , \quad (I.1.1)$$

then, according to Hearmon ⁽²³⁾, the elastic constants are related by

$$\left. \begin{aligned} c_{14} &= \beta_{13}^2 \beta_{23} \beta_{33} c_{33}^0 \\ c_{15} &= \beta_{13}^3 \beta_{33} c_{33}^0 \\ c_{24} &= \beta_{23}^3 \beta_{33} c_{33}^0 \\ c_{25} &= \beta_{13} \beta_{23}^2 \beta_{33} c_{33}^0 \\ c_{46} &= \beta_{13} \beta_{23}^2 \beta_{33} c_{33}^0 \\ c_{56} &= \beta_{13}^2 \beta_{23} \beta_{33} c_{33}^0 \end{aligned} \right\} + \text{terms in other } c_{ij}^0 \quad . \quad (I.1.2)$$

In order for these c_{ij} to vanish it is necessary that either $\beta_{13} = \beta_{23} = 0$ or $\beta_{33} = 0$. These are equivalent, respectively, to the requirements that either x_3 be parallel to X_3 or x_3 be perpendicular to X_3 . In effect this reduces the problem from a study of three dimensional rotations to a study of one dimensional rotations.

It is easily proven that under a rotation of x_1 and x_2 about x_3 both Types I and II elastic constants transform into either Types I or II elastic constants. For the case of x_3 parallel to X_3 , it is sufficient to consider only those standard elastic constants which are Type I or II and to rotate x_1 and x_2 about $x_3 = X_3$ to find other orientations of the coordinates for which the elastic constants c_{ij} are Type I or II. For the case of x_3 perpendicular to X_3 , first choose $x_1 = X_3$ and rotate x_3 in the X_1X_2 plane through an angle ϕ . Second, for each angle ϕ for which the elastic constants were found to be Type I or II, rotate x_1 and x_2 about x_3 to find the remaining orientations of the coordinates for which the elastic constants are Type I or II.

I.2. Examples of Type I Elastic Constants

I.2.1. Hexagonal Crystals

If the x_3 axis is along the c axis, then

$$c_{ij} = c_{ij}^{\circ} \quad (I.2.1)$$

If the x_3 axis is in the basal plane and the x_1 axis is along the c axis, the c_{ij} are related to the c_{ij}° by

$$[c_{ij}] = \begin{bmatrix} c_{33}^{\circ} & c_{13}^{\circ} & c_{13}^{\circ} & 0 & 0 & 0 \\ & c_{11}^{\circ} & c_{12}^{\circ} & 0 & 0 & 0 \\ & & c_{11}^{\circ} & 0 & 0 & 0 \\ & & & \frac{1}{2}(c_{11}^{\circ} - c_{12}^{\circ}) & 0 & 0 \\ & & & & c_{44}^{\circ} & 0 \\ & & & & & c_{44}^{\circ} \end{bmatrix} \quad (I.2.2)$$

I.2.2 Cubic Crystals

If the x_1 and x_3 axes are along cube edges, then

$$c_{ij} = c_{ij}^{\circ} \quad (I.2.3)$$

If the x_3 axis is along a face diagonal and the x_1 axis along a cube edge, then

$$[c_{ij}] = \begin{bmatrix} c_{11}^{\circ} & c_{12}^{\circ} & c_{12}^{\circ} & 0 & 0 & 0 \\ & c_{11}^{\circ} + c^{\circ} & c_{12}^{\circ} - c^{\circ} & 0 & 0 & 0 \\ & & c_{11}^{\circ} + c^{\circ} & 0 & 0 & 0 \\ & & & \frac{1}{2}(c_{11}^{\circ} - c_{12}^{\circ}) & 0 & 0 \\ & & & & c_{44}^{\circ} & 0 \\ & & & & & c_{44}^{\circ} \end{bmatrix}, \quad (1.2.4)$$

where

$$c^{\circ} = c_{44}^{\circ} - (c_{11}^{\circ} - c_{12}^{\circ})/2 \quad (1.2.5)$$

1.3. Numerical Values of Elastic Constants

The numerical values of the standard elastic constants and magnitudes of the Burgers vector of partial dislocations used in this report are given in Table 5. The values of b_p were computed from data in W. B. Pearson, Handbook of Lattice Spacings^p and Structures of Metals and Alloys, Pergamon Press, 1958. There is usually some uncertainty in the last digit given of both b_p and c_{ij}° ; reference should be made to the original literature for probable ^p errors. The values are for a temperature of 25°C, except for Zn of 22°C.

The elastic constants of graphite have been computed from the data of Riley⁽²⁵⁾ and of Bowman and Krumhansl⁽²⁶⁾. From Riley's results, recomputed with the more recent compressibility of Kabalkina and Vereshchagin⁽²⁷⁾, we get

$$\begin{bmatrix} c_{11}^{\circ} + c_{12}^{\circ} = 148.2 \times 10^{11} \text{ dynes/cm}^2 \\ c_{13}^{\circ} = 10.87 \\ c_{33}^{\circ} = 4.58 \end{bmatrix}. \quad (1.3.1)$$

From Bowman and Krumhansl

$$\begin{bmatrix} c_{11}^{\circ} + c_{12}^{\circ} = 141. \times 10^{11} \text{ dynes/cm}^2 \\ c_{12}^{\circ} = 28.2 \\ c_{44}^{\circ} = 0.23 \end{bmatrix}. \quad (1.3.2)$$

The values given in Table 5 are an average of these two sets of data.

TABLE 5
 NUMERICAL VALUES FOR ELASTIC CONSTANTS AND BURGERS VECTORS
 (c_{ij} in units of 10^{11} dynes/cm²)

| Element | b_p | c_{11} | c_{12} | c_{44} | c_{13} | c_{33} | Ref |
|------------------|---------|----------|----------|----------|----------|----------|-----|
| Graphite | 1.421 A | 116. | 29. | 0.23 | 10.9 | 4.66 | 1 |
| Be | 1.320 | 29.23 | 2.67 | 16.25 | 1.4 | 33.64 | 2 |
| Cd | 1.720 | 11.52 | 3.972 | 2.025 | 4.053 | 5.122 | 3 |
| Co | 1.447 | 30.71 | 16.50 | 7.55 | 10.27 | 35.81 | 4 |
| Mg | 1.853 | 5.928 | 2.590 | 1.632 | 2.157 | 6.135 | 5 |
| Zn | 1.538 | 16.368 | 3.646 | 3.879 | 5.30 | 6.347 | 6 |
| TiB ₂ | | 69. | 41. | 25. | 32. | 44. | 7 |
| Ag | 1.668 | 12.397 | 9.341 | 4.613 | | | 8 |
| Al | 1.653 | 10.732 | 6.094 | 2.832 | | | 9 |
| Au | 1.665 | 19.221 | 16.279 | 4.202 | | | 10 |
| Cu | 1.475 | 16.809 | 12.145 | 7.511 | | | 11 |
| Ni | 1.439 | 25.3 | 15.6 | 12.3 | | | 12 |
| Pb | 2.021 | 4.66 | 3.92 | 1.44 | | | 13 |
| TiC | | 50.0 | 11.3 | 17.5 | | | 7 |

1. See text.
2. J. F. Smith and C. L. Arbogast, *J. Appl. Phys.* 31, 99 (1960).
3. C. W. Garland and J. Silverman, *Phys. Rev.* 119, 1218 (1960).
4. H. J. McSkimin, *J. Appl. Phys.* 26, 406 (1955).
5. S. Eros and C. S. Smith, *Acta Met.* 9, 14 (1961).
6. G. A. Alers and J. R. Neighbours, *J. Phys. Chem. Solids* 7, 58 (1958).
7. J. J. Gillman and B. W. Roberts, *J. Appl. Phys.* 32, 1405 (1961).
8. R. Bacon and C. S. Smith, *Acta Met.* 4, 337 (1956).
9. R. E. Schmunk and C. S. Smith, *J. Phys. Chem. Solids* 9, 100 (1959).
10. W. B. Daniels and C. S. Smith, *Phys. Rev.* 111, 713 (1958).
11. R. E. Schmunk and C. S. Smith, *Acta Met.* 8, 396 (1960).
12. R. M. Bozorth, W. P. Mason, and H. J. McSkimin, *Bell System Tech. J.* 30, 970 (1951).
13. I. H. Swift and E. P. T. Tyndall, *Phys. Rev.* 61, 359 (1942).

BIBLIOGRAPHY

1. J. D. Eshelby, W. T. Read, and W. Shockley, *Acta Met.* 1, 251 (1953).
2. A. J. E. Foreman, *Acta Met.* 3, 322 (1955).
3. A. N. Stroh, *Phil. Mag.* 3, 625 (1958).
4. A. Seeger and G. Schöck, *Acta Met.* 1, 519 (1953).
5. G. Leibfried and H. D. Dietze, *Z. Physik* 126, 790 (1949).
6. G. W. De Wit, thesis, Univ. of Illinois, 1959; see also G. De Wit and J. S. Koehler, *Phys. Rev.* 116, 1113 (1959).
7. F. E. Fujita and K. Izui, *J. Phys. Soc. Japan* 16, 214 (1961).
8. T. Tsuzuku, *J. Phys. Soc. Japan* 12, 778 (1957); *Proc. Third Carbon Conf.*, 1957, (Pergamon Press, New York, Publ. 1959), p. 433.
9. S. Amelinckx and P. Delavignette, *Phys. Rev. Letters* 5, 50 (1960).
10. M. Peach and J. S. Koehler, *Phys. Rev.* 80, 436 (1950).
11. W. T. Read, *Dislocations in Crystals* (McGraw-Hill Book Company, Inc., New York, 1953), p.131.
12. A. Seeger, *Encyclopedia of Physics* (Springer-Verlag, Berlin, 1955), Vol. VII, Part 1, pp. 604-610.
13. S. Amelinckx and P. Delavignette, *J. Appl. Phys.* 31, 2126 (1960).
14. S. Amelinckx and P. Delavignette, paper presented at the AIME annual meeting, Feb. 26 - March 2, 1961, at St. Louis, Missouri (to be publ.); *Abs. in J. Metals* 13, 80 (1961).
15. M. J. Whelan, *Proc. Roy. Soc. (London)* A249, 114 (1959).
16. G. K. Williamson, *Proc. Roy. Soc. (London)* A257, 457 (1960).
17. R. Siems, P. Delavignette, and S. Amelinckx, *Z. Physik* (to be publ.). See also reference (14).
18. P. Delavignette and S. Amelinckx, *J. Nuclear Materials* 5, 17 (1962).
19. See the discussion and references in A. Seeger, *Encyclopedia of Physics* (Springer-Verlag, Berlin, 1955), Vol. VII, Part 1, pp. 560-563.
20. J. D. Eshelby, *Phil. Trans. Roy. Soc. (London)* A244, 87 (1951).
21. A. K. Head, *Proc. Phys. Soc. (London)* B66, 793 (1953).

BIBLIOGRAPHY CONT'D.

22. Charles S. Smith, Solid State Physics, edited by F. Seitz and D. Turnbull (Academic Press, Inc., New York, 1958) Vol. 6, p. 175.
23. R. F. S. Hearmon, Acta Cryst. 10, 121 (1957).
24. D. S. Lieberman and S. Zirinsky, Acta Cryst. 9, 431 (1956).
25. D. P. Riley, Proc. Phys. Soc. (London) 57, 486 (1945).
26. J. C. Bowman and J. A. Krumhansl, J. Phys. Chem. Solids 6, 367 (1958).
27. S. S. Kabalkina and L. F. Vereshchagin, Soviet Phys. - Doklady 5, 373 (1960); Doklady Akad. Nauk S.S.S.R. 131, 300 (1960).